Journal of South American Earth Sciences 131 (2023) 104536

Contents lists available at ScienceDirect

Journal of South American Earth Sciences

journal homepage: www.elsevier.com/locate/jsames

Orosirian-Stenian evolution of the Bolivian Precambrian Shield, SW Amazonian Craton, constrained by U–Pb geochronology and Nd–Hf isotopic parameters

Ramiro Matos [a,*], Wilson Teixeira [b], Amarildo S. Ruiz [c], Jorge S. Bettencourt [b], Mauro C. Geraldes [d], Gabriela Vargas-Mattos [e], Leticia Redes [f]

[a] Instituto de Investigaciones Geológicas y del Medio Ambiente, Universidad Mayor de San Andrés, Calle 27, Pabellón Geología, Campus Universitario Cota Cota, La Paz, Bolivia

[b] Instituto de Geociências, Universidade de São Paulo, Rua do Lago 562, Cidade Universitária, 05508-080, São Paulo, SP, Brazil

[c] Faculty of Geosciences, Federal University of Mato Grosso, Brazil

[d] Faculdade de Geologia, Universidade do Estado do Rio de Janeiro, Rua São Francisco Xavier 524, 20559-900, Rio de Janeiro, RJ, Brazil

[e] Yacimientos Petrolíferos Fiscales Bolivianos, Carr. Paraguay, s/n, Bilbao, Villamontes, Bolivia

[f] Instituto de Geociências, Universidade de Brasília, Asa Norte, Brasília, DF, 70910-900, Brazil

ARTICLE INFO

Keywords:
Bolivian Precambrian Shield
Paleo- and Mesoproterozoic
Zircon U–Pb ages
Nd and zircon Hf constraints
Amazonian Craton

ABSTRACT

We present new and compiled U–Pb zircon ages and Hf zircon and Nd constraints for rocks of the Bolivian Precambrian Shield southwestern fringe of the Amazonian Craton. The database and updated geologic information provide new insights into the Orosirian-Early Stenian evolution. This shield can be subdivided into the San Diablo and Paraguá domains considering their particular geologic histories and lithostratigraphic units: i) the southern San Diablo Domain consists mainly of amphibolite facies gneissic rocks with documented ages as old as 1940 Ma, intruded by the Correreca, Santo Corazón, Tauca, and Santa Terezita plutons with documented ages between 1874 and 1849 Ma; ii) the Paraguá Domain comprises the Lomas Maneches Granulite Complex (1820 Ma), the Chiquitania meta igneous-sedimentary complex (1750-1690 Ma), and the roughly coeval San Ignacio Schist Group (1690 Ma). Locally, the country rocks are crosscut by the Yarituses Suite (1683-1610 Ma), which is contemporary with the Lomas Maneches Granitoid Suite (1690-1660 Ma). The Pensamiento Granitoid Complex (1440-1270 Ma), constituted by syn-to late-kinematic and late-to post-kinematic granites, collectively known as San Ignacio Granitoids, is widespread in the studied region. Six zircon U–Pb datings and 76 compiled data determine that the continental crust experienced a long-lived tectonic-magmatic history, distinguished by three accretionary events: 1941–1849 Ma, 1690-1610 Ma, and 1430-1340 Ma. These events have relationships with the Proterozoic growth of Amazonia enclosing the distal Rio Apa Terrane. Later, the southern portion of the Bolivian Precambrian Shield experienced crustal shortening, magmatism, and overprints due to the Sunsás/Greenville (1200-1000 Ma) orogeny that marks the Amazonia-eastern Laurentia collage in Rodinia times. From a petrogenetic perspective, the country rocks of the San Diablo Domain yield documented Sm–Nd T_{DM} ages and ε_{NdT} values of ca. 1.69 to 2.29 Ga and −5.7 to +1.8 respectively, suggestive of the derivation of short-lived protoliths. The Correreca intrusion (1874–1862 Ma) gives published zircon Hf model ages of 2.68 Ga and 2.29 Ga and coupled ε_{HfT} values of −4.6 to +2.8. The bulk isotopic signature for the San Diablo rocks is consistent with magma genesis in a moderately juvenile-like accretionary arc, where the calc-alkaline types show a subduction-related signature. In contrast, the country rocks in the adjoining Paraguá Domain show published Sm–Nd T_{DM} model ages of ca. 1.55 to 2.48 Ga and ε_{NdT} values of −4.9 to +5.2, pointing to distinct protoliths in the magma genesis. The Yarituses Suite includes the following granites: La Cruz (1673 ± 21 Ma), Refugio (1673 ± 25 Ma; 1641 ± 4 Ma), San Pablo (1609 ± 17 Ma), San Miguel (1681 ± 13 Ma), and Rosario (1678 ± 21 Ma). These granites yield variable Sm–Nd T_{DM} model ages of ca. 1.67 to 2.48 Ga and ε_{NdT} of +4.1 to −3. 8 (Ta ble 1), suggesti ng the derivation of distinct crustal components. The new and compiled data demonstrate first time that the Lomas Maneches and Yarituses suites, in conjunction with the Chiquitania complex and the newly dated

* Corresponding author.
E-mail addresses: rmatoss@yahoo.com (R. Matos), wteixeir@usp.br (W. Teixeira), asruiz@gmail.com (A.S. Ruiz), jsbetten@usp.br (J.S. Bettencourt), geraldes@uerj.br (M.C. Geraldes), glvarg@ypfb.gob.bo (G. Vargas-Mattos), leticiaredes@hotmail.com (L. Redes).

https://doi.org/10.1016/j.jsames.2023.104536
Received 7 November 2022; Received in revised form 7 August 2023; Accepted 8 August 2023
Available online 31 August 2023
0895-9811/© 2023 Elsevier Ltd. All rights reserved.

Ambaybo rhyolite (1691 ± 8 Ma) of the San Ignacio Schist Group, belong to a distinct tectonic-magmatic episode akin to an active continental margin. The Pensamiento Granitoid Complex (1440-1270 Ma) shows documented Sm–Nd T_{DM} model ages between ca. 1.55 and 2.42 Ga and predominantly crustal-like isotopic signatures as low as −4.6 typical of a continental arc setting. On a broader scale, the San Ignacio Granitoids are products of the Alto Guaporé orogeny, previously established in the Brazilian counterpart, characterized by an accretionary phase (ca. 1440 Ma) and a collisional one (ca. 1330 Ma) against the active margin of proto-Amazonia at the Ectasian. The regional structural framework of those plutons in the Bolivian counterpart suggests that the San Ramón and Coronación granodiorites (1429-1423 Ma) are pre-to syn-kinematic to the collisional phase. In contrast, the La Junta (1380 ± 17 Ma) and San Martin (1409 ± 17 Ma) granites are syn-to-late kinematic. The Diamantina granite (1357 ± 19 Ma) is coeval with the Alto Guaporé collisional phase, while the San Andrés granite (1289-1275 Ma) is a post-kinematic pluton. The ε_{NdT} of the Pensamiento Granitoid Complex varies from +5.2 to −4.6. The onset of the Sunsás orogeny, characterized by an allochthonous collisional-type belt (1.2–1.0 Ga) ends the polycyclic evolution of the Bolivian Precambrian Shield, leading to tectonic stability of the Amazonian Craton.

1. Introduction

The Amazonian Craton (Fig. 1) consists of an ancient core bounded by Proterozoic tectonic provinces that exhibit progressively younger orogenic episodes toward the southwest. The youngest one is the ca. 1.2–1.0 Ga Sunsás collisional orogeny which aligns with the Grenville orogeny, eventually assembling the Western Amazonia and Eastern Laurentia to form the Rodinia Supercontinent (e.g., Tohver et al., 2005, 2006; Cordani and Teixeira, 2007; Cordani et al., 2009; Teixeira et al., 2010; Nedel et al., 2021). The SW portion of the Amazonian Craton includes the Central Brazil Shield enclosing the Precambrian crust of Bolivia (Fig. 1, inset). This region hosts segments of orogenic belts to which the Rio Negro-Juruena (1.82–1.60 Ga), Rondonian-San Ignacio (1.59–1.30 Ga), and Sunsás-Aguapeí (1.20–0.95 Ga) provinces are tectonically related. Their potential tectonic correlation with the adjoining Rio Apa Terrane and the Paraguá Terrane (Bolivia) in Paleo-to Mesoproterozoic times (Cordani and Teixeira, 2007; Teixeira et al., 2020; Ribeiro et al., 2020, 2022a, 2022b; Nedel et al., 2020; Redes et al., 2020), are still under debate. The Juruena accretionary orogeny (1.81–1.51 Ga), formed the Juruena and Jamari terranes (Scandolara et al., 2017). These are regionally represented by predominantly calc-alkaline and alkaline felsic plutonic-volcanic rocks and roughly coeval volcano-sedimentary units. The eastern portion of the Juruena crust also hosts an ancient crustal remnant (2.05–2.03 Ga), intruded by granitoid suites (1.99–1.93 Ga and 1.89–1.87 Ga) – Fig. 1. Rizzotto et al. (2019) argued that an intracontinental LIP-like plutonic, volcanic belt generated between 1.82 and 1.76 Ga would be the most outstanding feature of the Juruena crust. Reis et al. (2021) proposed the term Alta Floresta SLIP for some calc-alkaline volcanic and granitic rocks emplaced over a short-lived period of 10 million years into the Juruena crust between 1.80 and 1.79 Ga. The Juruena-Jamari crusts document two metamorphic episodes dated at ca. 1.69–1.63 Ga (high-grade collisional metamorphism) and 1.42–1.37 Ga (e.g., Bettencourt et al., 2010; Teixeira et al., 2010; Scandolara et al., 2017). The Jamari Terrane (after Scandolara et al., 2017) is herein considered tectonically related to the Rondonian-San Ignacio Province, given the widespread Mesoproterozoic reworking and recurrent magmatism (Bettencourt et al., 2010).

The Juruena polycyclic crust correlates well with the Precambrian rocks of Bolivia and the distal Rio Apa Terrane - RAT (Fig. 1), The RAT comprises two arc-type terranes limited by a significant thrust shear lineament (e.g., Teixeira et al., 2020; Ribeiro et al., 2020, 2022a, 2022b). The Western Domain comprises the Porto Murtinho Complex (2.10–1.94 Ga) and the Amoguijá (1.90–1.82 Ga) continental belt, with isotopic constraints indicative of protoliths as old as 2.7 Ga. Granitoid rocks are widespread in the Eastern Domain akin to the Caracol juvenile accretionary belt (1.82–1.74 Ga) and the associated Alto Tererê back-arc basin (ca. 1.79 Ga). Ribeiro et al. (2022b) established a petrogenetic link between the RAT, Paraguá Terrane, and Amazonian Craton, inferred by a robust set of zircon U–Pb–Hf isotopic data. They consider the Western Domain of the RAT, the San Diablo Domain in Bolivia, and the Ventuari-Tapajos Province (2.00–1.80 Ga) to contain crustal reworking magmatism developed during an advancing episode of the Paleoproterozoic accretionary orogen of the RAT. In their model, the younger Eastern Domain, the Paraguá Domain, and the Rio Negro-Juruena province derived from crustal growth in a retreating episode of this accretionary orogen.

The Rondonian-San Ignacio Province (Fig. 1) originated from multiple accretionary arcs (1.59–1.35 Ga), partly reworking the Jamari and Alto Jauru terranes (Bettencourt et al. (2010). The Alto Guaporé orogeny evolved from (1.47–1.45 Ga (accretionary phase) to 1.35–1.33 Ga (collisional phase) as a belt (e.g., Rizzotto et al., 2013), is the most prominent tectonic element in the region (Fig. 1) with a relict fossil suture zone (Trincheira ophiolite). This orogeny produced widespread granitogenesis across SW Amazonia (Cordani and Teixeira, 2007; Bettencourt et al., 2010; Rizzotto et al., 2013, 2014), including the San Ignacio Granitoids (Pensamiento Granitoid Complex) in the Bolivian Precambrian Shield. The Alto Guaporé orogeny marks the eventual suturing of the Paraguá Terrane against the Rio Negro-Juruena Province at ca. 1.35 Ga (e.g., Bettencourt et al., 2010; Teixeira et al., 2010), a model followed here.

The Rondonian-San Ignacio and the Rio Negro-Juruena provinces experienced collision-related deformation and tectonic reactivations related to the Sunsás 1.20–1.00 Ga orogeny (Teixeira et al., 2010; Nedel et al., 2020; Redes et al., 2020; Ribeiro et al., 2020, 2022a, 2022b), manifested by the Sunsas belt and the associated sedimentary and metasedimentary sequences, as well by the Rincón del Tigre mafic to ultramafic complex (Fig. 1). The Sunsás dynamics is roughly coeval with inboard crustal shortening, transpression, and magmatism within, both, the Nova Brasilândia metasedimentary belt (1.13–1.00 Ga) within the Rondonian-San Ignacio Province. Intra-plate (≤1.0 Ga) A-type granitoid suites, mafic dikes, and nearby shear zones represent the late tectonic to anorogenic offshoots over the cratonic margin (Teixeira et al., 2010, 2015a; Quadros et al., 2021). .

The Bolivian Paraguá Terrane is adjacent (current coordinates) to the Rio Negro-Juruena and Rondonian-San Ignacio provinces and representative hosts units of the Sunsás-Aguapeí Province. It is genetically related to the accretionary growth of SW Amazonia with the intervening RAT, as evidenced by the Nd and Hf isotopic constraints (Cordani and Teixeira, 2007; Teixeira et al., 2020; Ribeiro et al., 2020, 2022a, 2022b). Noteworthy, the accretionary growth is contemporary with inboard intraplate volcanic plutonic phenomena within the already established domains, such as the Uatumã (1.89–1.87 Ga) and Alta Floresta (1.80–1.79 Ga) SLIP events among other tectonic overprints (Cordani et al., 2010; Teixeira et al., 2019a and b; Rizzotto et al., 2013; Reis et al., 2021).

Paleogeographic correlations of the Paraguá Terrane and its tectonic features, like the San Diablo front are still open. These models invoke some distal crustal remnants and blocks, largely overlain by recent sedimentary covers or by Andean rocks, such as Arequipa (Peru),

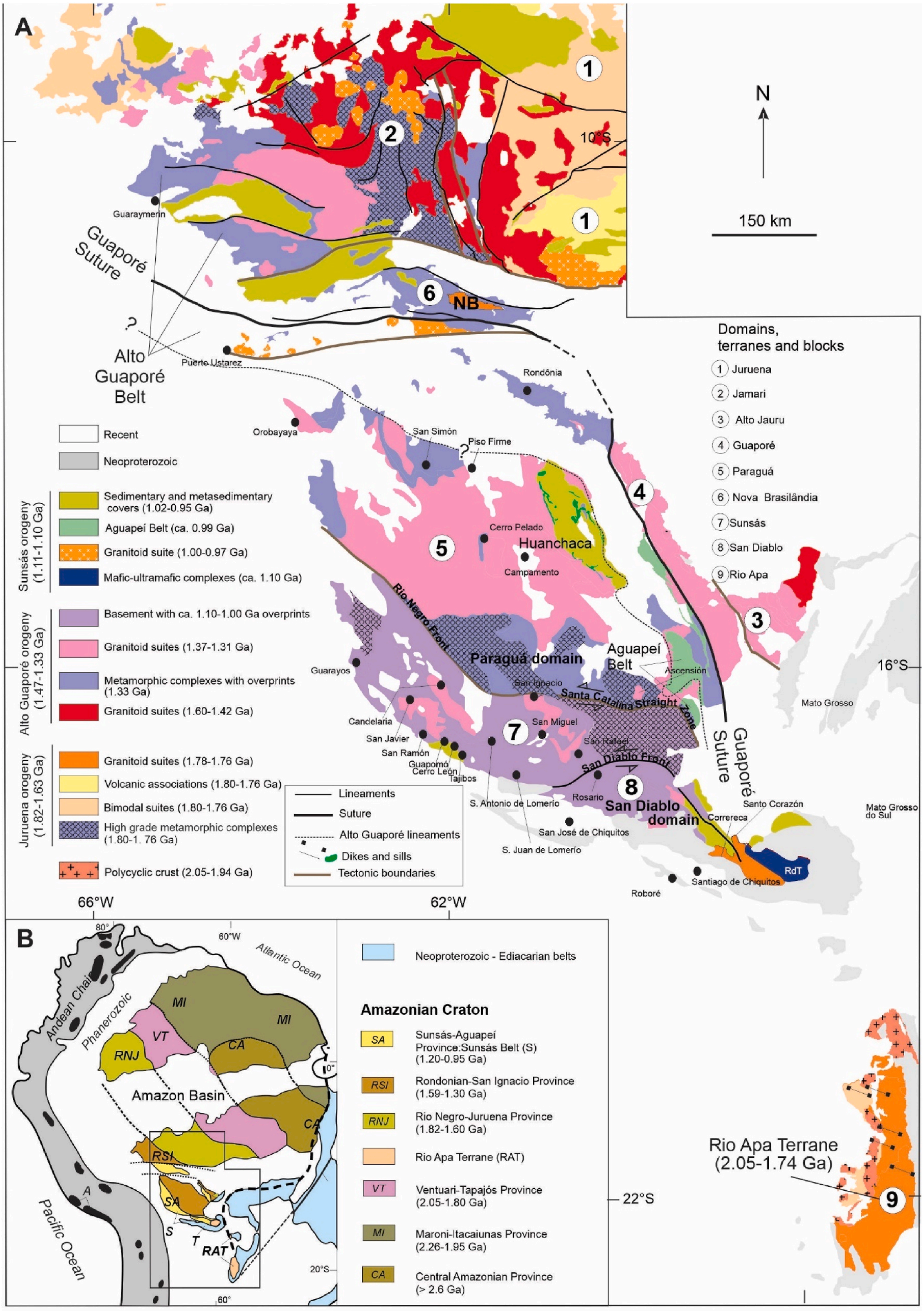

Fig. 1. A) Geologic outline of the SW Amazonian Craton shows the north-to-south domains, terrains, and blocks. Keys: 1 Roosvelt-Juruena; 2 Jamari; 3 Alto Jauru; 4 Guaporé; 5 Paraguá; 6 Nova Brasilandia; 7 Sunsás; 8 San Diablo; 9 Rio Apa. Geologic framework adapted from Cordani et al. (2010), and Teixeira et al. (2019b, 2020). B) tectonic sketch of the Amazonian Craton. The Andean chain's basement inliers (reworked in the late Mesoproterozoic) are also black (A = ca. 2.0 Ga-old Arequipa Terrane). See text for details.

Table 1
Summary of SHRIMP U–Pb, Sm–Nd, Rb–Sr, and K–Ar ages of selected rocks of the Bolivian Precambrian shield.

Sample	Unit/local	East	North	Composition/rock	Sm	Nd	$^{147}Sm/^{144}Nd$	$^{143}Nd/^{144}Nd$	$\varepsilon_{(0)}$	T_{DM} (Ga)	$\varepsilon_{(T1)}$	Hf Model age (Ga)	$\varepsilon_{(Hf)}$	U/Pb magmatic	U/Pb inherited	U/Pb metamorphic	Rb–Sr	References
Yarituses suite																		
601	San Pablo	641,522	8,108,107	Peraluminous, medium-K	13	57.49	0.137	0.51185	−15	2.48	−2.5 to −3.8			1609 ± 17				Vargas-Mattos (2010)
JO12	Refugio	571,410	8,200,548		3.4	23.5	0.087	0.51168	−19	1.67	+4.1			1641 ± 4	1668 ± 8			Santos et al. (2008)
408	Refugio	569,780	8,200,723	Peraluminous, high-K*	2.81	17.01	0.1	0.51161	−20	1.92	+0.2							This work
SR83	Refugio	560,190	8,202,119	Peraluminous, high-K*										1673 ± 25				This work
558	La Cruz	564,815	8,172,721	Metaluminous, low-K*	11.4	60.58	0.1137	0.51184	−12	1.83	+2.1			1673 ± 21				This work
LR19	Rosario	753,226	8,087,279	Metaluminous, calc-alkalic to alkali-calcic	6.05	31.37	0.1165	0.51054	−16	1.89	+0.9	2.34, 1.82	−0.9 + 8.9	1678 ± 21		1390		Redes (2021)
SM08	San Miguel	661,792	8,114,201	Metaluminous calc-alkalic to alkali-calcic	4.71	27.48	0.1036	0.51059	−18	1.81	+1.9	2.32, 1.88	+0.3 + 6.9	1681 ± 13		1320 ± 19		Redes (2021)
SR20	Sujalito	568,875	8,161,113		20.3	101.1	0.1212	0.51056	–	1.87	+1.8			1682 ± 3				Nedel et al. (2021)
547	Sujalito	568,433	8,160,690	Metaluminous, low-K*	15.6	86.3	0.1099	0.51184	−16	1.77	−0.8							This work
Lomas Maneches suite																		
	San Jorge			Gneiss										1658 ± 15				Matos et al. (2014)
240	Lomas Maneches	775,298	8,142,135	Granite										1663 ± 13	1755 ± 70	1320 ± 11		Boger et al. (2005)
261	Lomas Maneches	754,315	8,127,041	Granite										1689 ± 5	1773 ± 50			Boger et al. (2005)
San Ignacio Schist Group																		
1402	Ambaybo	573,588	8,154,440	Rhyolite										1691 ± 8				This work
221D	San Ignacio	734,798	8,164,135	Schist										1764 ± 6**				Boger et al. (2005)
Chiquitanía Gneiss Complex																		
551	Momené	492,607	8,223,228	Metaluminous, high-K*	21.9	96.48	0.137	0.5122	−8.5	1.67	+1.6							This work
532	Victoria	598,307	8,247,676	Peraluminous, high-K*	16.9	91.04	0.1121	0.51178	−17	1.88	−2.3							This work
JO8	Las Madres	614,641	8,234,660	Gneiss	16	91.03	0.1064	0.51174	−18	1.86	−4.9			1678 ± 11**		1118 ± 15		Santos et al. (2008)
JO9	Las Madres	610,986	8,230,206	Gneiss	10.4	57.2	0.1104	0.51162	−20	1.74	−0.6							Santos et al. (2008)
JO16	Río Branco	552,779	8,188,759	Gneiss	2.1	14.7	0.0864	0.51159	−20	1.58	+0.9							Santos et al. (2008)
235 A	Chiquitania	749,798	749,798	Gneiss/Schist										1764 ± 12				Boger et al. (2005)
235A1	Chiquitania	749,798	749,798	Gneiss/Schist										1690**		1336 ± 6		Boger et al. (2005)
IM06 1223**	Miraflores	758,232	8,102,485	Gneiss Nedel et al. (2017)										1745 ± 21				
IM07 1274**	Miraflores	758,232	8,102,485	Gneiss Nedel et al. (2017)										1883 ± 43				
IM04C	Miraflores	758,232	8,102,485	Gneiss										1685 ± 5		1111 ± 10		Nedel et al. (2017), 2020
LR02A	Miraflores	758,232	8,102,485	Gneiss	2.75	20.15	0.0824	0.51052	–	1.86	+1.1							Nedel (2020)
	Miraflores	758,232	8,102,485	Peraluminous, calc-alkalic to alkali-calcic	1.92	11.03	0.105	0.51025	−23	2.15	−2.4			1747 ± 11	1813	1425 ± 32		Redes (2021)
Lomas Maneches Granulite Complex																		
514	Chontita1	661,421	8,297,922	Peraluminous, high-K*	17.1	111.6	0.0928	0.51159	−21	1.83	−2.9							This work
515	Chontita2	661,080	8,294,234	Metaluminous, low-K*	7.03	36.48	0.1166	0.51162	−20	2.24	−2.8							This work
518	Rio Negro	574,116	8,298,963	Metaluminous, high-K*	17.2	100.6	0.1031	0.5118	−16	1.71	−0.4							This work
528	Silvestre	588,374	8,275,158	Peraluminous, high-K*	0.54	4.08	0.0801	0.51152	−22	1.73	+3.0							This work
531	San Pastor	599,344	8,255,173	Peraluminous, high-K*	3.11	17.04	0.1105	0.51177	3.11	1.88	+1.0							This work
JO3	LManechis	231,887	8,182,323	Granulite	3.94	21.94	0.1086	0.51164	−20	2.07	+0.5			1818 ± 13	1874 ± 9	1339 ± 4		

(*continued on next page*)

Table 1 (*continued*)

Sample	Unit/local	East	North	Composition/rock	Sm	Nd	$^{147}Sm/^{144}Nd$	$^{143}Nd/^{144}Nd$	$\varepsilon_{(0)}$	T_{DM} (Ga)	$\varepsilon_{(T1)}$	Hf Model age (Ga)	$\varepsilon_{(Hf)}$	U/Pb magmatic	U/Pb inherited	U/Pb metamorphic	Rb–Sr	References
***		Santos et al. (2008)																
	Lomas Maneches Granulite Complex														1961	Litherland et al., 1986		
San Diablo domain																		
1329	Correreca	294,918	8,002,625	Peraluminous, calc-alkaline	9.48	52.91	0.1083	0.5115	−22	2.08	−1.2			1861 ± 8				Redes et al. (2020)
820	Correreca	288,681	8,001,692	Peraluminous, calc-alkaline	8.32	50.41	0.0998	0.51141	−24	2.12	−0.8	2.68; 2.29	−4.6; +2.8	1861 ± 7				Redes et al. (2020)
822	Correreca	294,907	8,002,622	Peraluminous, calc-alkaline	9.33	53.1	0.1062	0.51151	−22	1.96	−0.5							Redes et al. (2020)
820	Correreca	288,681	8,001,692	Peraluminous, medium-K						2.8	−8.5			1925 ± 32 (Pb–Pb)				Vargas-Mattos et al. (2010)
821	Correreca	293,265	8,002,475	Peraluminousmedium-K						2.9	−9.4			1894 ± 13				Vargas-Mattos et al. (2010)
822 A	Correreca	294,907	8,002,622	Peraluminous,medium-K														Vargas-Mattos et al. (2010)
822 B	Correreca	294,907	8,002,622	Peraluminous,medium-K														Vargas-Mattos et al. (2010)
822C	Correreca	294,907	8,002,622	Peraluminous,medium-K														Vargas-Mattos et al. (2010)
ST02	Santa Terezita	765,314	8,014,207	Peraluminous, alcali	7.6	42.82	0.1073	0.51163	−20	1.96	+1.8			1849 ± 11	2212 ± 77			Redes et al. (2020)
ST03	Santa Terezita	767,294	8,013,958	Peraluminous, calc-alkaline	8.77	45.53	0.1165	0.51167	−19	2.08	+0.2			1853 ± 5				Redes et al. (2020)
ID09	Tauca	217,835	8,038,079		8.76	46.91	0.1128	0.51047	−22	2.29	−1.8			1852 ± 3				Nedel et al. (2021)
1328	Santo Corazon	308,865	8,111,975	Peraluminous, calc-alkaline	5.37	32.03	0.1014	0.51141	−24	2.14	−1.1							Redes et al. (2020)
824	Santo Corazon	305,036	8,009,769	Peraluminous, calc-alkaline	5.64	32.01	0.1065	0.51139	−24	2.27	−2.7			1874 ± 15				Redes et al. (2020)
ID08	Las Tojas	210,847	8,090,710	Gneiss	2.84	20.93	0.0820	0.511592			−5.7			1941 ± 40		1271		Nedel (2020); Nedel et al. (2021)

** = detrital; *** = monazite; rhy = rhyolite.

Pampia (Ramos, 2009; Ramos et al., 2010; Ramos, 2018; Mišković et al., 2009), or even a hypothetical Paleoproterozoic block embracing basement units older than 1.7 Ga in Peru, Argentina and Bolivia (Casquet et al., 2012).

This paper addresses the tectonic evolution of the Paraguá Terrane with an emphasis on the Statherian and Ectasian periods. Based on new and compiled isotopic-chemical data of the lithostratigraphic units of the San Diablo and Paraguá domains (Bolivia), the available structural information, correlative tectonic-magmatic episodes within SW Amazonian Craton, are discussed, supported by robust U–Pb geochronology Sm–Nd and Hf constraints, and strong trace-element geochemical characterization (Nedel et al., 2020, 2021; Redes et al., 2020; Ribeiro et al., 2020, 2022a, 2022b (see Figs. 1 and 2). We also consider the geophysical airborne and satellite information for characterizing the tectonic role of particular granitoid suites unraveling the evolution of the accretionary margin of proto-Amazonian Craton.

2. Precambrian geology of Bolivia revisited

The geology of the Bolivian Precambrian shield is outlined in Fig. 2 based on updated geologic information, manifested by the orogenic episodes regionally termed Sunsás and San Ignacio orogenies and the basement units. A compilation of available zircon U–Pb age determinations is also shown. The continental crust is essentially composed of Paleo-to Mesoproterozoic rocks represented by widespread granitoid and gneissic rocks and relicts of metasedimentary sequences

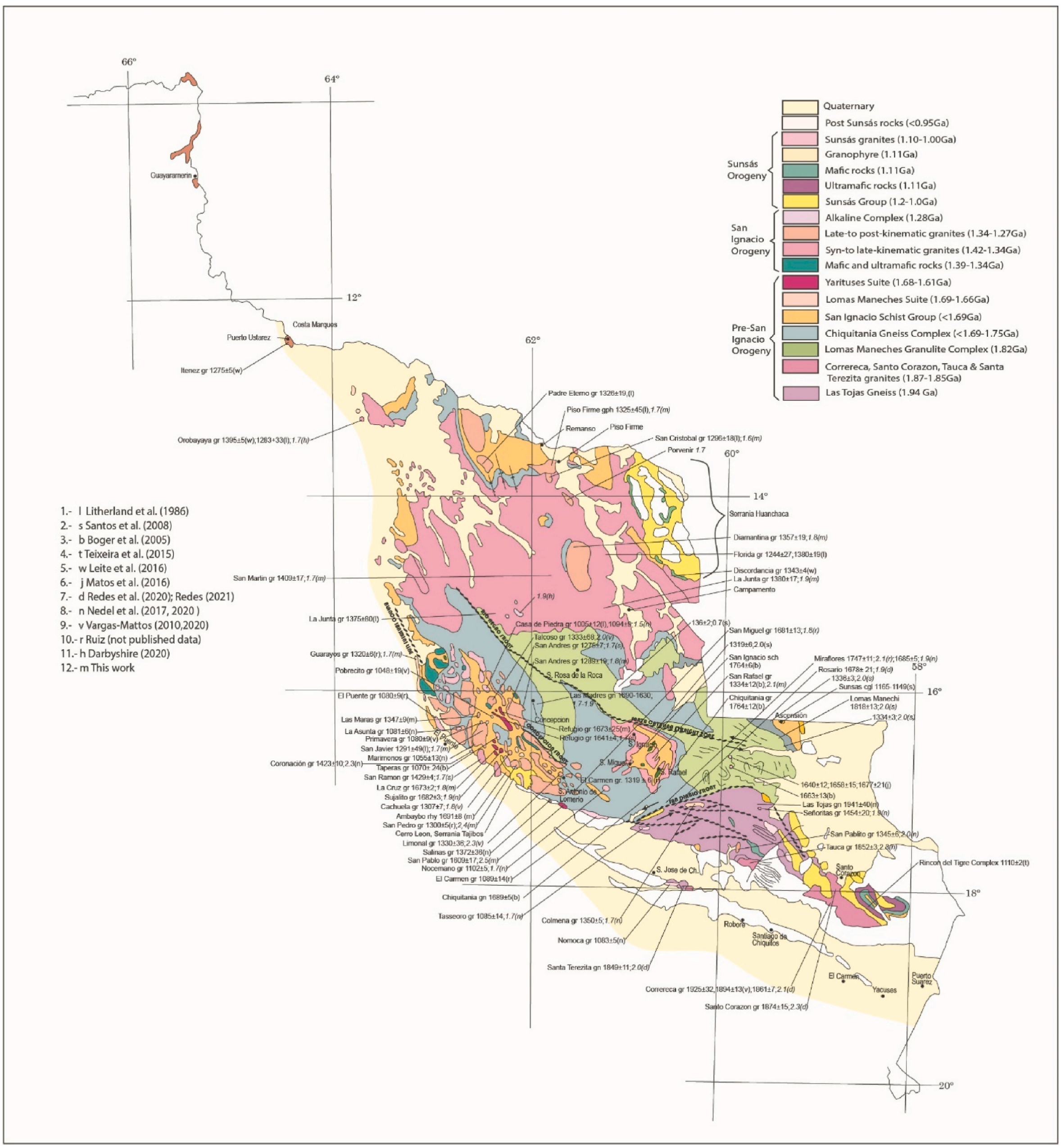

Fig. 2. Geochronological map showing main geologic units: the Paraguá domain (LMGC, CGC, and SISG), San Diablo domain granites e.g., Santo Corazon, Correreca, Tauca, and Santa Terezita; the Yarituses Suite, Pensamiento granitoid Complex and the Sunsás granites and the Sunsás Group, modified after Litherland et al. (1986). Structural trends are shown schematically: the Blanco Ibaimini Line, the Conception Front, The San Diablo Front, the Rio Negro Front, and the Santa Catalina Straight Zone. The San Diablo Front separates two areas: the Paraguá domain on the northern part shows disharmonic and asymmetrical first-order folds. In contrast, the San Diablo domain on the south portrays anastomosed lenticular shear zones enclosing unsheared nuclei rocks. T_{DM} data is in italics.

(e.g., Litherland et al., 1986; Matos Salinas, 2010 and references therein; Bettencourt et al., 2010; Cordani et al., 2010; Teixeira et al., 2010, 2020; Santos et al., 2008; Nedel et al., 2020; Redes et al., 2020; Ribeiro et al., 2020, 2022a, 2022b).

The Paraguá Craton (Litherland et al., 1986 for a review), also termed Paraguá Terrane, has been considered an allochthonous terrane that accreted along the active margin of proto-Amazonian Craton during the Mesoproterozoic (e.g., Boger et al., 2005; Cordani and Teixeira, 2007; Bettencourt et al., 2010).

The Concepción, Rio Negro, and San Diablo are the most prominent shear zones across the Bolivian Precambrian Shield (Litherland et al., 1986), as follows: i) the Concepcion Front, as part of the Sunsás belt, is a branch of the Rio Negro Front and together with the secondary shear zones follows an NW trend, as a straight zone (Fig. 2), outlined by radiometry and magnetometry maps (Adamek et al., 1996). It separates high metamorphic-grade rocks on the NE side of granites and rocks of lower metamorphic grade on the SW (Fletcher, 1979). ii) the Rio Negro Front and the Santa Catalina Straight Zone separate the Paraguá Terrane on the northern part of the Sunsás belt on the south (e.g., Litherland et al., 1986). The Rio Negro Front has a weak expression and color in composite satellite imagery, consisting of SE trending mylonitic rocks. iii) the Santa Catalina Straight Zone follows an E-W trend of the left-lateral shear zone, and magnetic anomalies define its eastern side (Alcocer and Claure, 2000). iv) the San Diablo Front is a prominent curvilinear feature distinguishable from satellite images, separating the San Diablo Domain on the south of the Sunsás belt on the north, both with different aged metamorphic rocks and structures. For instance, the shear zones at the San Diablo Front enclose thin bands of sheared schists containing lenticular cores of unsheared rocks. The main rock types in the shear zone are represented by mylonite augen gneiss and ultra-mylonites. Some rotated phenoblasts indicate left-lateral shear sense (Landivar and Gonzalez, 1997; Matos, 2010). Northward of the San Diablo Domain, granites like the Casa de Piedra, Taperas, and Naranjito (Fig. 2) are associated with the Sunsás belt (Nedel et al., 2020). The reactivation of the San Diablo Front is likely related to the Sunsás collisional offshoots, as suggested by the available K–Ar muscovite dates of 1067 to 868 Ma (Darbyshire, 1979). Indeed, the southern Sunsás belt shows NNW transport direction manifested by the left-lateral transcurrent fault represented by the curvilinear shear zone of the San Diablo Front (Fig. 1).

2.1. Geology of the San Diablo domain

The San Diablo Domain (Fig. 2) is the oldest substratum, as indicated by the U–Pb ages - Table 1. For instance, the Las Tojas gneiss yielded a crystallization age of 1941 ± 40 Ma, the oldest record documented in the area. The Señoritas granite was intrusive into the Las Tojas gneiss and yielded 1415 ± 30 Ma crystallization age. In contrast, the inherited zircon gave a period of 1954 ± 51 Ma, which suggests that Las Tojas gneiss is the potential protolith (Nedel et al., 2020).

The San Diablo Domain also hosts the Correreca granodiorite, initially described by Mitchell (1979). This pluton yielded preliminary U–Pb zircon evaporation ages of 1894 ± 24 Ma and 1925 ± 32 Ma (Vargas-Mattos et al., 2010) – see Fig. 2. More recently, Redes et al. (2020) reported U–Pb LA-ICPMS zircon ages for several plutons within this domain, as follow: The Correreca granodiorite is high-K calc-alkalic to alkali-calcic and peraluminous in composition. It yielded 1861 ± 7 Ma, and the coupled Sm–Nd T_{DM} values ranged from 2.12 to 1.96 Ga with ε_{NdT} values of −0.5 and −1.2 (Table 1). The zircon Hf isotopic constraints indicated negative to positive ε_{HfT} values of −4.6 to +2.8 and Hf model ages of 2.68 and 2.29 Ga (Table 2), suggesting a continental arc signature. The Santo Corazón granite is calc-alkalic and peraluminous in composition. It yielded a crystallization age of 1874 ± 15 Ma similar to the Correreca granodiorite, and Sm–Nd T_{DM} ages of 2.27 and 2.14 Ga and ε_{NdT} values of −1.1 and −2.7 (Table 1). Similarly, the Santa Terezita gneiss is calc-alkalic to alkaline and peraluminous in composition. It gave an age of 1849 ± 11 and 1853 ± 5 Ma, Sm–Nd T_{DM} ages of 2.08 and 1.96 Ga, and juvenile-like ε_{NdT} of +0.2 and + 1.8. (Table 1). The bulk isotopic signature for these three plutons suggests the role of juvenile and crustal components in the magma genesis, such as expected for an evolved magmatic arc setting during which the San Diablo crust was formed (Redes et al., 2020).

The Tauca granite is medium-K calc-alkalic, peraluminous in composition, with volcanic arc affinity (See Supplementary Table T1). It yielded 1852 ± 3 Ma having, therefore, an age match with the Correreca and Santo Corazon granitic rocks (Nedel et al., 2021; Redes et al., 2020)- the Sm–Nd T_{DM} ages of 2.29 Ga and ε_{NdT} of −1.84. The San Pablito granite is high-K calc-alkalic, peraluminous in composition, with a within-plate affinity (See Supplementary Table T1). Nedel (2020) reported a crystallization age of 1345 ± 6 Ma, whereas one inherited zircon with $^{207}Pb/^{206}Pb$ age of ca. 1848 Ma suggests components like the Tauca granite in the magma genesis.

The Colmena granite (Table 1) located to the west is high-K calc-alkalic, peraluminous in composition, and with a within-plate affinity (See Supplementary Table T1) and yielded a crystallization age of 1350 ± 5 Ma (Nedel et al., 2017) identical to that of the San Pablito granite of 1345 ± 6 and T_{DM} ages between 1.86 and 1.69 with ε_{NdT} of −2.4 and + 0.4 (Fig. 2). The San Diablo Domain hosts several mafic igneous rocks and amphibolites in contrast to the northern portion of the Paraguá Domain. The metamorphism reached amphibole facies at 1320 Ma.

2.2. Geology of the Paraguá Domain

The Paraguá Domain is essentially composed of Mesoproterozoic rocks and Orosirian-age crust. It comprises distinct lithostratigraphic units, namely of the older to the younger: The Lomas Maneches Granulite Complex (LMGC), The Chiquitania Gneiss Complex (CGC), The San Ignacio Schist Group (SISG), the Lomas Maneches Suite, and the Yarituses Suite.

1) The LMGC is the oldest basement unit, as inferred from a preliminary Rb–Sr whole rock array in several samples with ca. 1.96 Ga (Litherland et al., 1986). This complex consists of intercalated thin bands of granulite with gneisses containing hypersthene or cordierite. It occupies large portions of the shield (Fig. 2), occurring at Carmen de Ruiz and Lomas Maneches massifs. The granulites are

Table 2
Nd and Hf analytical data for selected rocks of the Bolivian Precambrian Shield.

Sample	Unit/local	East	North	Geochemical signature	Tectonic setting	$_{HfT}$ Model age (Ga)	ε_{HfT}	T_{DM} (Ga)	ε_{NdT}	References
Yarituses suite										
LR19	Rosario	753,226	8,087,279	Metaluminous, calc-alkalic to alkali-calcic	VAG	2.34, 1.82	−0.9 + 8.9	1.89	+0.9	Redes (2021)
SM08	San Miguel	661,792	8,114,201	Metaluminous calc-alkalic to alkali-calcic	VAG	2.32, 1.88	+0.3 +6.9	1.81	+1.9	Redes (2021)
San Diablo domain										
820	Correreca	288,681	8,001,692	Peraluminous, calc-alkaline	VAG	2.68, 2.29	−4.63, +2.76	2.12	−0.8	Redes et al. (2020)

Table 3
Summary of the main granite rocks of the Pensamiento Granitoid Complex from the Precambrian Shield of Bolivia.

Sample	Unit/local	East		Geochemical signature	Sm	Nd	$^{147}Sm/^{144}Nd$	$^{143}Nd/^{144}Nd$	$\varepsilon_{(0)}$	T_{DM} (Ga)	$\varepsilon_{(T1)}$	U/Pb magmatic	U/Pb inherited	U/Pb metamorphic	Rb–Sr/ K–Ar	References
Paraguá Domain																
	Florida														*1244 ± 27*	Litherland et al., 1986
1414	Itenez	340,255	8,628,825									1275 ± 5				Leite et al. (2016)
JO10	San Andrés	581,172	8,205,825		14.8	77.9	0.1149	0.511963	−13.5	1.68	−0.15	1275 ± 7	1331 ± 13			Santos et al. (2008)
404	San Andrés	591,538	8,202,865	Peraluminous, médium-K*	30.76	161.51	0.1152	0.51188	−14.9	1.80	−1.60	1289 ± 19	1616 ± 18			This work
502	San Cristobal	623,561	8,479,249	Metaluminous, high-K	7.83	32.43	0.1459	0.512337	−5.87	1.58	+2.75				*1296 ± 18*	Litherland et al., 1986; Matos et al. (2009)
503	San Cristobal	625,100	8,474,329	Metaluminous, high-K	9.65	40.46	0.1442	0.512316	−6.28	1.59	+2.63					Matos et al. (2009)
412	San Pedro	580,114	8,156,767	Peraluminous, médium-K *	8.71	34.06	0.1547	0.512111	−10.3	2.42	−4.57					This work
	San Pedro	579,673	8,156,775									1300 ± 5				A. Ruiz, unpub. data, 2019
413	Cachuela	576,414	8,165,706	Peraluminous, médium-K	9.08	53.34	0.1030	0.511781	−16.73	1.73	−0.79	1307 ± 7				Vargas-Mattos, 2010, 2020
535	El Carmen	608,143	8,186,921	Metaluminous, high-K*	19.1	126.59	0.0913	0.512027	−11.9	1.26	+5.22					This work
538	Santa Rosario	611,545	8,161,667	Peraluminous, high-K*	14.56	73.08	0.1205	0.512177	−8.99	1.41	+3.40					This work
	El Carmen	601,673	8,177,166									1319 ± 6				A. Ruiz, unpub. data, 2019
540	Coloradillo	618,959	8,151,123		17.84	91.03	0.1185	0.51187	−14.9	1.9	−1.7					This work
545	Monterito	609,480	8,152,641		17.93	94.91	0.1143	0.51188	−14.6	1.9	−0.6					This work
JO18	Santa Rita	–			28.9	142.38	0.1227	0.511883	−15.1	1.96	−2.57	1319 ± 6	1746 ± 21			Santos et al. (2008)
552	Guarayos	478,345	8,243,122	Peraluminous, médium-K*	12.33	63.24	0.1179	0.511954	−13.4	1.73	+0.05					This work;
GY7	Guarayos	492,393	8,246,668									1320 ± 6				A. Ruiz, unpub. data 2019;
501	Piso Firme	635,174	8,493,483	Metaluminous, high-K	6.83	30.37	0.136	0.512229	−7.99	1.59	+2.32				1325 ± 45	Litherland et al., 1986; Matos et al. (2009)
	Padre Eterno	–													*1326 ± 19*	Litherland et al., 1986
543	Limonal	629,430	8,142,042	Peraluminous, médium-K	10.51	49.3	0.1289	0.511978	−12.9	1.90	−1.64					This work
544	Limonal	629,430	8,142,042	Peraluminous, médium-K	7.54	32.07	0.1421	0.511964	−13.15	2.30	−3.86	1330 ± 36				Vargas-Mattos (2010), 2020
546	S. Rafaelito	591,975	8,160,598	Peraluminous, high-K*	7.66	39.52	0.1172	0.511926	−13.9	1.76	−0.37					This work
549	Limones	535,349	8,180,169	Peraluminous, high- K*	7.87	74.16	0.0642	0.51142	−23.8	1.65	−1.23					This work
418	Talcoso	559,723	8,221,524	Peraluminous, médium-K	10.02	47.46	0.1277	0.511927	−13.88	1.97	−2.14	1333 ± 68				Vargas-Mattos (2010), 2020
JO5	Lomas Manechi	230,795	8,174,544		9.73	49.78	0.1182	0.511764	−17.4	2.06	−3.97			1334 ± 3		Santos et al. (2008)
JO6	Rio Fortuna	205,805	8,194,212		8.78	45.03	0.1179	0.511761	−17.1	2.06	−3.83	1336 ± 3	1753 ± 10			Santos et al. (2008)

(*continued on next page*)

Table 3 (*continued*)

Sample	Unit/local	East		Geochemical signature	Sm	Nd	$^{147}Sm/^{144}Nd$	$^{143}Nd/^{144}Nd$	$\varepsilon_{(0)}$	T_{DM} (Ga)	$\varepsilon_{(T1)}$	U/Pb magmatic	U/Pb inherited	U/Pb metamorphic	Rb–Sr/ K–Ar	References
228	San Rafael											1334 ± 12	1686 ± 16			Boger et al. (2005)
406	San Rafael	745,786	8,152,306	Peraluminous, high-K*	12.77	63.76	0.1211	0.51179	−16.6	2.1	−3.72					This work
	San Javier														1291 ± 49	Litherland et al., 1986
PNK72	Discordancia	739,665	8,388,670	Peraluminous, high-K*								1343 ± 4				Leite et al. (2016)
LM81	Las Maras	543,798	8,204,379	Peraluminous, high-K*								1347 ± 9				Matos- Salinas (2010)
403	San Javier	554,034	8,100,387	Peraluminous, high-K*	1.98	15.76	0.0763	0.51152	−21.8	1.69	−1.31					This work
504	Porvenir	652,858	8,445,140	Peraluminous, high-K	19.27	79.09	0.1474	0.512285	−6.89	1.74	+1.48					Matos et al. (2009)
505	Diamantina	661,416	8,392,512	Peraluminous, high-K	10.66	63.26	0.1019	0.511834	−15.7	1.65	+0.39					Matos et al. (2009)
506	Diamantina	662,257	8,385,235	Peraluminous, high-K	12.87	78.69	0.0989	0.511789	−16.6	1.66	+0.03					Matos et al. (2009)
507	Diamantina	660,633	8,375,785	Peraluminous, high-K	13.27	70.13	0.1145	0.511859	−15.2	1.82	−1.25	1357 ± 19				Matos et al. (2009)
508	Diamantina	659,133	8,367,145	Peraluminous, high-K	5.73	23.61	0.1469	0.512202	−8.51	1.92	−0.06					Matos et al. (2009)
510	La Junta	661,952	8,342,071	Peraluminous, calc-alkaline	18.73	99.73	0.1135	0.511727	−17.8	2.01	−3.66					Matos et al. (2009)
511	La Junta	662,399	8,324,281	Peraluminous, calc-alkaline	14.69	80.73	0.11	0.51172	−17.9	1.95	−3.21					Matos et al. (2009)
512	La Junta	681,586	8,312,847	Peraluminous, calc-alkaline	3.6	22.02	0.0988	0.511636	−19.6	1.87	−2.94	1380 ± 17	1486 ± 18		1375 ± 80	Litherland et al., 1986; Matos et al. (2009)
513	La Junta	662,091	8,309,042	Peraluminous, calc-alkaline	18.69	100.57	0.1124	0.511685	−18.6	2.04	−4.29					Matos et al. (2009)
SM10	Salinas	621,135	8,119,055									1372 ± 36	1684 ± 110			Nedel et al. (2021)
509	San Martín	642,451	8,367,213	Peraluminous, high- K	25.35	107.63	0.1424	0.512257	−7.43	1.68	+1.78	1409 ± 17		1318 ± 14		Matos et al. (2009)
	Florida														*1380 ± 19*	Litherland et al., 1986
	Orobayaya									1.73					1283 ± 33	Litherland et al., 1986; Darbyshire (2000);
1417	Orobayaya	419,113	8,537,476									1395 ± 5				Leite et al. (2016)
ID11	Coronación	536,591	8,176,805		2.08	17.47	0.0719	0.510918	–	1.55	+2.26	1423 ± 10	1815, 1876	1405		Nedel (2020); Nedel et al. (2021)
401	San Ramón	552,489	8,262,872	Peraluminous, calc-alkaline*	7.65	53.74	0.0861	0.51159	−20.5	1.73	−0.29					This work
JO14	San Ramón	552,489	8,262,872		7.66	57.86	0.0801	0.511677	−18.8	1.57	+2.32	1429 ± 4***				Santos et al. (2008)
San Diablo Domain																
ID02	San Pablito	193,334	8,058,067	Metaluminous, high-K*	9.45	47.26	0.1209	0.510768	−15.7	1.97	−2.72	1345 ± 6	1848			Nedel (2020); Nedel et al. (2021)
IM33	Colmena	772,073	8,104,879		10.62	56.97	0.1127	0.510814	−16.1	1.84	−2.11					Nedel (2020)
IM34	Colmena	772,419	8,101,560		4.24	20.66	0.1241	0.510939	−11.7	1.69	+0.43	1350 ± 5	1635, 1761			Nedel (2020); Nedel et al. (2021)
IM35	Colmena	768,693	8,103,643		0.75	4	0.113	0.511801	−16.3	1.86	−2.39					Nedel (2020)

(*continued on next page*)

Table 3 (*continued*)

Sample	Unit/local	East		Geochemical signature	Sm	Nd	$^{147}Sm/^{144}Nd$	$^{143}Nd/^{144}Nd$	$\varepsilon_{(0)}$	T_{DM} (Ga)	$\varepsilon_{(T1)}$	U/Pb magmatic	U/Pb inherited	U/Pb metamorphic	Rb–Sr/ K–Ar	References
TA88	Colmena	776,258	8,106,261	Peraluminous, high- K*												This work
DM516	Señoritas	214,362	8,080,743	Peraluminous, high- K*	3.51	20.68	0.1027	0.511532	−21.6	2.08	−5.27		/			This work
ID06	Señoritas	214,002	8,080,868		1.42	8.75	0.0984	0.51091	–	1.95	−6.52	1415 ± 30	1954 ± 51			Nedel (2020); Nedel et al. (2021)

***= monazite; *K–Ar, italic.*

charnockitic, enderbitic, and basic hypersthene-bearing rocks associated with biotite-garnet gneisses (e.g., Litherland et al., 1986). Further U–Pb zircon work defined a more confident age for the LMGC of 1818 ± 13 Ma and a metamorphic overprint dated at 1340 Ma (Santos et al., 2008) - (Table 1).

2) The CGC, which broadly encompasses the LMGC across the southern portion of the Paraguá Domain, consists mainly of amphibolite facies. These partly migmatitic, ortho-para-derived gneisses exhibit characteristic interference folding. The main regional lithotype is a pale pink to gray, banded (medium-to coarse-grained), micaceous quartz-feldspathic gneiss. The Chiquitania rocks are as young as 1685–1689 Ma (Boger et al., 2005; Santos et al., 2008; Nedel et al., 2017; Redes et al., 2020) (Table 1). For instance, a hornblende-biotite granitoid rock yielded a U–Pb crystallization age of 1689 ± 5 Ma with inherited zircon of 1830 Ma. The less discordant data produced a $^{207}Pb/^{206}Pb$ age of 1333 ± 6 Ma, interpreted as a partial melting episode, pointing to a crustal reworking episode (Boger et al., 2005). According to these authors, the U–Pb provenance constraints indicated that these paragneiss rocks were primarily derived from a 1764 ± 6 Ma crustal source and were deposited after 1690 Ma. Santos et al. (2008) also reported U–Pb zircon detrital ages of the Las Madres paragneiss (CGC) varying from 1690 to 1630 Ma and three metamorphic zircon overgrowth with 1350, 1317, and 1118 Ma. (Fig. 2). The Sm–Nd T_{DM} ages in different CGC rocks range between 2.15 and 1.67, whereas the ε_{NdT} values vary from −4.9 to +1.6 (Table 1).
3) The SISG crops out as discrete metavolcanic-sedimentary occurrences across the Paraguá Domain (Fig. 2). These exposures are composed of metapsamites, schists, phyllites, slates, mafic metatuffs, BIF, metachert, metalavas of tholeiitic and felsic composition, akin to an oceanic setting. The SISG rocks exhibit transitional contacts with the Chiquitania lithotypes, suggesting they might be a single lithostratigraphic unit with Barrovian metamorphic zoning (Litherland et al., 1986). Similarly, additional geologic surveys (Adamek et al., 1996; López-Montaño and y Bernasconi, 1988) on the metavolcanic-sedimentary occurrences between the Concepcion Front and the Blanco-Ibaimini Lineament suggest they may represent a single regional-scale entity, at least 250–300 km long and 60–85 km wide (see Fig. 2). We provide a first age constraint for the San Ignacio Group, referred to the Ambaybo rhyolite in Section 4.
4) The Lomas Maneches Suite (Boger et al., 2005) - LMGS - is an igneous suite previously ascribed to the LMGC of Litherland et al. (1986). The emplacement of this suite is contemporary with the Chiquitania and San Ignacio Group, according to the literature data (Boger et al., 2005). These authors considered that the Lomas Maneches Suite consists mainly of orthopyroxene-bearing granitoid sills that are interleaved with minor metasedimentary rocks of calc-silicate or psammitic composition, croppíng out east of San Rafael (see Fig. 2). The granitoid sills yielded a U–Pb age in zircon cores of 1663 ± 13 Ma, inferred as the emplacement age. Additional analyses of the zircon rims yielded an age of 1320 ± 11 Ma (Table 1), interpreted as the time of partial melting (Boger et al., 2005). Besides this, Matos et al. (2014) reported U–Pb ages between 1677 and 1640 Ma for granitoid rocks at Las Rengas close to the boundary between Bolivia and Brazil (Fig. 2). Furthermore, a foliated gneiss on the central-western part of the San Diablo Front yielded 1685 ± 5 Ma (Nedel et al., 2017; Redes et al., 2020) matching U–Pb ages documented by Matos et al. (2014) and Boger et al. (2005).
5) The granitoid rocks of the Yarituses Suite (Matos, 2012) occur along the southwestern fringe of the Paraguá Domain, exemplified by the San Pablo, Refugio, La Cruz, Sujalito, San Miguel, and Rosario plutons (Tables 1 and 2) as follows: The San Pablo body coincides with the San Diablo lineament, and it underwent shearing during the Sunsás orogeny (see item 2.1). The LA-ICP-MS data yield an average age of 1609 ± 17 Ma (MSWD = 4.6) (Vargas Mattos, 2010). The Sujalito granite is a greyish-orange rock that crops east of San Ramon

(Fig. 2). It is oriented NNW parallel to the shear zones that overprint the SISG. It has two zircon populations, rounded and elongated crystals that gave 1682 ± 3 Ma (Nedel et al., 2020). Santos et al. (2008) reported SHRIMP U–Pb ages in zircon, monazite, and titanite for the Refugio syenogranite occurring near San Javier (Table 1; Fig. 2). According to these authors, two zircon populations are present. The youngest one, dated at 1641 ± 4 Ma, and an inherited one, formed at 1668 ± 8 Ma. Finally, Redes (2021) documented additional isotopic data for the San Miguel and Rosario gneisses (Fig. 2), considered part of the Yarituses suite. The first one (Fig. 2) indicated a crystallization age of 1681 ± 13 Ma, with Sm–Nd T_{DM} values of 1.81 and an ε_{NdT} value of +1.9. The coupled zircon Hf model ages yielded 2.32 and 1.88 Ga with ε_{HfT} values + 0.3 and + 6.9. The Rosario gneiss produced 1678 ± 21 Ma, with the Sm–Nd T_{DM} values of 1.89 and ε_{NdT} of +0.92. The Hf model age yielded 2.34 and 1.82 Ga with ε_{HfT} values of −0.9 and + 8.9 (see Tables 1 and 2). Both plutons are, therefore, mainly mantle-derived. From a tectonic point of view, these plutons fit an accretionary setting for the Yarituses Suite, similar to the genetically related Lomas Maneches Granitoid Suite.

2.3. San Ignacio granitoids

The Pensamiento Granitoid Complex (PGC) (Litherland et al., 1986) represents the San Ignacio granitoid rocks besides granophyres widespread in the Paraguá Domain. Some PGC plutons (i.e., tonalites and granodiorites) also occur within the San Diablo Domain (see section 2.1). First Rb–Sr and K–Ar dates documented for such "syn-tectonic" granites yielded values between 1400 and 1250 Ma (Litherland et al., 1986) – Table 3. More recent U–Pb ages indicated that the plutonic pulses lasted from 1455 to 1270 Ma (Santos et al., 2008; Matos et al., 2014). Noteworthy, the published U–Pb dates align with the magmatic activity of the Alto Guaporé orogeny (1.44–1.33 Ga) – see section 1.

These granitoid rocks in Bolivia can be distinguished into two groups according to the deformation features and compositions (Fig. 2). The granitic rocks like the San Martin and La Junta plutons are syn-to late-kinematic with Do3 regional deformation, time-related with Mesoproterozoic PGC generation. They present amphibolite facies and show distinct shapes concerning the regional foliation of the country rocks. Similarly related to the Do3 phase, the San Martín and La Junta granites - the most extensive of the PGC - are weakly foliated to augen gneiss showing a planar tectonic fabric appearance with biotite flakes and prismatic hornblende and containing K- feldspar phenocrysts of 1.5–3 cm long (Hawkins, 1982). In contrast, the late-to post-kinematic plutons (San Cristobal and Porvenir) are structurally discordant to the regional foliation, showing circular or elliptical shapes emplaced into the syn-to late-kinematic bodies like the Diamantina into the San Martin granite. In some places, penecontemporaneous crosscutting relationships can be observed. According to the structural inferences, the San Andrés and Itenez granites (ca. 1.27 Ga; Table 3) may be late-kinematic to post-kinematic (Figs. 2 and 3).

Matos et al. (2009) reported major, trace, and REE chemical analyses in the northern area of the PGC (e.g., La Junta, San Martin, Diamantina, Porvenir, San Cristobal, and Piso Firme granitic bodies). These rocks are sub-alkaline to high-K calc-alkaline, peraluminous, and fractionated LREE/HREE, consistent with a magmatic arc signature. Similarly, the Guarayos, Talcoso, Cachuela, and Limonal granites are late-to post--kinematic. The Cachuela, Talcoso, and Motacusal (Limonal) granites show

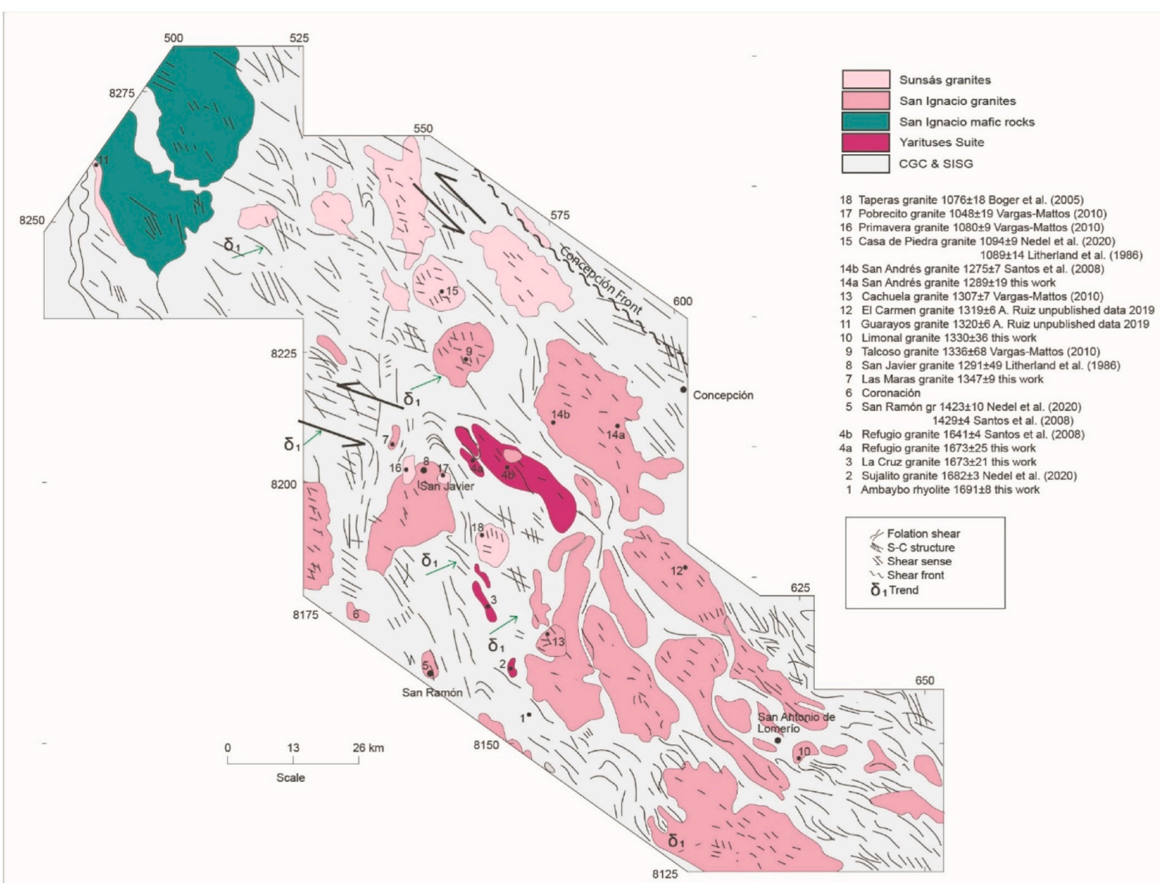

Fig. 3. Structural map of Concepción Sheet area interpreted of the composite image of airborne radiometric and magnetic data. It shows the Yarituses Suite, the Pensamiento Granitoid Complex, and Sunsás granites, foliated by Sunsás northwest trend left-lateral shear sense and S–C structure into a hosted rock belonging to the Chiquitania Gneiss Complex and San Ignacio Schist Group. The green arrow shows the principal σ_1 stress trend corresponding to an oblique tectonic.

SiO2 content of 70–75%. The Talcoso and Limonal are peraluminous, whereas Cachuela is peraluminous to metaluminous (Vargas Mattos et al., 2020). We discuss later the tectonic implications of such geochemical features. These bodies yielded Sm–Nd T_{DM} ages of 2.42 to 1.55 Ga, whereas the ε_{NdT} values range from −4.3 to +2.8 (Table 3). The Discordancia monzogranite (1343 Ma) with a rapakivi-type texture (Litherland, 1982; Leite et al., 2016) located on the border of Bolivia and Mato Grosso state (Fig. 2) shows a high-K calc-alkalic signature, peraluminous in composition, and within plate affinity (see Supplementary Table T1).

2.4. San Ignacio - type granitoid in the brazilian counterpart

Bettencourt et al. (2014), and Leite et al. (2016) documented three distinctive felsic igneous suíte in the Costa Marques region: Ouro Fino (OFIS, 1347 ± 9 Ma), São Domingos (SDIS, 1057 ± 10 Ma, and Costa Marques (CMIS, 998 ± 10 Ma). Two additional samples from SDIS yield SHRIMP U–Pb zircon ages of 1086 ± 12 Ma and 1754 ± 22 Ma (alkali-feldspar granite), and 1083 ± 6 Ma and 1375 ± 7 Ma (quartz-syenite porphyry). The 1086 ± 12 and 1083 ± 6 Ma are interpreted as the crystalization ages, and the1754 ± 22 Ma and 1375 ± 7 Ma as the inherited zircon age. The SDIS crystalization ages vary from 1086 Ma to 1057 Ma. Zircons from the 1347 Ma quartz-syenite (OFIS), 1086 to 1057 Ma granites and quartz-syenites (SDIS), and 998 Ma trachyte porphyry (CMIS) show ε_{HfT} = +0,1 to +2.9, −20.4 to +2.7 and −6.2 to +5.4, respectively, suggesting variable crustal and juvenile source contributions to the felsic magmas. The 1754 Ma and 1375 Ma inherited zircons show εHfT varying from −19.6 to −14.4, −1.9 to +0.8, and TDM (double stage) ranging from 3.6 to 2.3 Ga, and 2.1 Ga, respectively. Inherited zircon ages (1754 and 1375 Ma), and TDM (double stage) ages of all samples (3.6–1.5 Ga) indicate the involvement of Archean, Paleo-and Mesoproterozoic crusts for the felsic magma genesis. The authors (Bettencourt et al., 2014; Leite et al., 2016) suggest: 1- three magmatic events within the time interval of ca 350 Ma; 2- Variable crustal and mantle source components for the magma genesis; 3- Paleo-to Mesoproterozoic crustal source with probable contribution from Archean material; 4- the zircon Hf isotope signature yielded values between +0.1 and + 6.0, indicating the juvenile nature of these rocks -Table 4.

In the Mato Grosso state, the correlative plutons are the Lajes and Tarumã granites (1380-1310 Ma), whereas the Cascata, Passagem, Fronteira, Guaporei, and Morrinhos granites (1410-1280 Ma) crop out nearby the Vila Bela da Santíssima Trindade (See Table 5). From a tectonic perspective, all these plutons and their widespread occurrence suggest an outstanding granitization with crustal thickening produced by the Alto Guaporé orogeny, to which the PGC is also petrogenetically related.

3. Methods

3.1. Geochemistry

Sampling campaigns were carried out at different times along the Bolivian Precambrian Shield. On this occasion, the main petrographic units were recognized, and representative samples were taken. Thin sections were made and described for mineralogical and textural characterization at the Laboratory of Microscopy of San Andrés University. Geochemical analyses for major, minor, and trace elements were carried out at two laboratories: Patujú and Señoritas of the San Diablo Domain, Refugio, Sujalito and La Cruz of Yarituses Suite, San Ramón, San Javier, Discordancia, San Rafael, Limones, San Rafaelito, Guarayos, Santa Rosario, El Carmen, San Pedro and San Andrés of the San Ignacio Granites were analyzed at the Chemistry Laboratories of the Sao Paulo University. On the other hand, Tauca, San Pablito, and Colmena of the San Diablo Domain, Santa Rosa of Yarituses Suite, and Las Maras of the San Ignacio Granites were performed at ActLab of Canada. Santa Terezita, Santo Corazón, and Correreca granites were published by Redes et al. (2020). San Miguel and Rosario granites by Redes (2021). San Pablo, Talcoso, Limonal, and Cachuela were presented by Vargas-Mattos (2010). San Martín, La Junta, Diamantina Porvenir, Piso Firme, and San Cristobal by Matos et al. (2009) (see Fig. 5 a,b, and c). However, the geochemical nomenclature used for Paleoproterozoic supracrustal rocks has not been discussed in detail. Supplementary Table T1 presents the geochemical dataset of major, minor, and trace elements.

3.2. U–Pb isotopes

U–Pb zircon age determinations were primarily performed in the decade of 2000 using the ID-TIMS technique in multigrain fractions. Therefore these results are taken as an estimate due to the routine used. During the 2000 decade, additional SHRIMP age determinations were conducted on granitoid samples using different laboratories in Brazil and China. More recently, we carried out a SHRIMP analysis of volcanic rock of the SISG. The dating was carried out using a Sensitive High-mass Resolution Ion MicroProbe (SHRIMP-II) and the Thermo-Fisher Neptune

Table 4
Summary of the main geological units of Rondônia state.

.Unit	Lithology	Age (Ma)	ε_{NdT}	References
São Lourenço-Caripunas	Alkali-feldspar granite, syenogranite, quartz-syenite, and rhyolite porphyry	1314–1309		Bettencourt et al. (1997, 1999)
Ouro Fino		1347 ± 9		Bettencourt et al. (2014); Leite et al. (2016).
Alto Candeais	Monzogranite, syenogranite, charnockite, and syenite	1346–1338		Bettencourt et al. (1997, 1999)
Alto Escondido	Monzogranite and syenogranite			Quadros and Rizzotto (2007) Rizzotto and Quadros (2007)
Igarapé Enganado	Syenogranite, monzogranite, and granodiorite	1340	+2.8	Bettencourt et al. (2010)
Serra do Colorado	Anorthosite		+2.7	Quadros and Rizzotto (2007) Rizzotto and Quadros (2007)
Teotônio	Alkali-feldspar granite, quartz-alkali-feldspar syenite, minor syenogranite, quartz-syenite, monzogranite, diorite, monzodiorite, and monzonite.	1390–1360		Bettencourt et al. (1999, 2010)
Santo Antonio	Monzonite, syenogranite, quartz monzonite	1390–1360		Bettencourt et al. (2010)
Praia Alta	Biotite syenogranite	1436 ± 7; 1426 ± 5		Rizzotto et al. (2013)
Rio Piolho	Syenogranite	1442 ± 16		Rizzotto et al. (2013)
Rio Galera Complex	Tonalitic gneis	1459 ± 9		Rizzotto et al. (2013)
Trincheira Complex	Mafic granulite, amphibolite	1470–1430	+2.6 to +8.8	Rizzotto et al. (2013)
Colorado Complex	Dioritic gneiss	1469 ± 5		Rizzotto et al. (2013)
Rio Crespo	granitic gneiss and charnockitic granulite	1500	+1.0 to +1.8	Bettencourt et al. (2006)

Table 5
Geologic compilation of principal granites of Mato Grosso related to the Alto Guaporé orogeny.

Area	Granite	Lithology	Composition	Age	T_{DM} (Ga)	ε_{NdT}	References
Porto Espiridao	Lajes	Fine to medium-grained, leucocratic rock.	Sienogranite to monzogranite.	U–Pb zircon, 1310 ± 44 Ma	1.7	+3.4 to 0.0	Ruiz (2005)
	Tarumã	Pink porphyroclasts in green coarse-grained matrix.	Monzo to syenogranite; metaluminous to slightly peraluminous	LA-ICP-MS 1377 ± 5 Ma	1.9	Negative	Ruiz (2005); Matos et al. (2009)
Vila Bela da Santíssima Trindade	Cascata	Two facies: the western facies is coarse-grained, xenomorphic texture. The eastern facies is a porphyritic rock.	Western facies: tonalite to granodiorite; Eastern facies granodiorite to monzogranite.	Pb–Pb evaporation, 1412 ± 5 Ma			Cabrera et al. (2009a, 2009b)
	Passagem	Stocks, plugs, and dykes; hypidiomorphic inequigranular and xenomorphic texture; fine to medium-grained rock.	Monzo to syenogranite, rarely granodiorite. Calc-alkaline type, high potassium; slightly peraluminous	LA-ICP-MS, 1284 ± 20 Ma	1.6	−7	Jesus et al. (2010)
	Fronteira	Holocrystalline, leucocratic, and xenomorphic in texture	Monzogranite to granodiorite	Pb–Pb zircon evaporation, 1333 ± 4 Ma			Marcello et al. (2009); Ruiz et al. (2012)
	Guaporei	Coarse-grained and porphyritic.	Monzogranite to granodiorite, quartzmonzonite and syenogranite. Calc-alkaline type, metaluminous to peraluminous,	Pb–Pb zircon evaporation, 1314 ± 3 Ma	1.7		Nalon et al. (2013)
	Morrinhos	Inequigranular, medium to coarse-grained, locally porphyritic	Granodiorite to monzogranite; alkali-calc, metaluminous to slightly peraluminous; some features of A-type granite	U–Pb SHRIMP 1350 ± 12 Ma,	1.8	−2.57	França et al. (2014).

laser-ablation (LA) multi-collector inductively coupled plasma mass spectrometer (ICP-MS) at the Geochronological Research Center of the University of São Paulo (CPGeo-USP), Brazil. For this study, six samples of key rocks were dated and selected by relevant field relationships (Table 6). Further unpublished LA-ICPMS datings are also considered (Redes, 2021) for a more robust integrated interpretation.

La Junta (sample LJ20512) and San Martín (CA0509), Diamantina (CP30507), La Cruz (LC0558), and San Andrés (SA0404) granites were dated by U–Pb SHRIMP-II (Sensitive High-Resolution Ion Microprobe) at the Chinese Academy of Geological Sciences (Beijing). Representative zircon grains were handpicked at the Geochronological Research Center (CPGeo–USP) under a binocular microscope, mounted in an epoxy resin disc, and polished and coated with gold film. Zircons were photographed with transmitted and reflected light and cathodoluminescence (CL) images were obtained which are shown in Fig. 4b. Isotopic data were plotted on the Concordia diagram using isoplot (Ludwig, 2003). Compston et al. (1992) and Sato et al. (2014) described the analytical procedures of zircon using SHRIMP. Inter-element fractionation ion emission of zircon was corrected relative to the RSES reference TEMORA 1 (417 Ma; Black et al., 2003). The weighted mean ages are quoted at the 95% confidence level (2σ). All ages described in the text are weighted mean $^{207}Pb/^{206}Pb$ ages.

The zircon grains were separated according to the magnetic susceptibility, following the procedures of Krogh (1982). The grains were dissolved individually with HF, and the mixed tracer $^{205}Pb/^{235}U$ was added. Pb and U were separated into cation exchange columns according to the procedures described by Krogh (1973) and Parrish et al. (1987). Isotopic compositions were measured on a mass spectrometer with a thermal ionization of a solid source (Triton mass spectrometer using the Daly detector).

The Pb isotopic compositions were analyzed in simple Re filament using silica gel and phosphoric acid, similar to the respective UO^{2+} analyses. U fractionation was monitored by analysis of the NBS SEM U-500 standard. Uncertainties in the U/Pb ratio resulting from fractionation and mass spectrometry are around ±0.5%. The isotopic compositions of ^{208}Pb, ^{207}Pb, and ^{206}Pb radiogenic were calculated considering corrections for the Pb blank (<10 pg) and the non-radiogenic compositions of these isotopes. Modification used the model of Stacey and Kramers (1975). Uncertainties in the radiogenic Pb are in the order of ±0.1%. The errors generated by the uncertainty in the regression were calculated to be 2σ.

3.3. *Whole-rock Sm–Nd analyses*

Sm–Nd analyses were conducted on 24 samples at the Geochronological Research Center of the University of São Paulo (CPGeo-USP), Brazil; 13 from PGC, 3 from Yarituses Suite, 2 from CGC, 5 five from LMGC, and one from the San Diablo Domain (Table 7). Approximately 0.1 mg of powdered rock sample was dissolved in concentrated HNO_3, HF, and HCl. The isotope dilution got the Sm and Nd concentrations with a combined spike tracer using the two-column techniques described by Sato et al. (1995). The isotope ratios were measured on the VG-354 multi-collector mass spectrometer. During the analyses period, laboratory blanks of analyses yielded maximum values of 0.4 ng for Nd and 0.7 ng for Sm. The average $^{143}Nd/^{144}Nd$ for La Jolla standard was 0.511857 (46 analyses), with 2σ standard deviations reported in parentheses. The Sm–Nd T_{DM} model ages from one-stage (whole rocks) were calculated using model parameters after DePaolo (1981): a = 0.25, b = 3, c = 8.5 as well as $^{143}Nd/^{144}Nd = 0.7219$ to normalize the isotope ratios [$^{143}Nd/^{144}Nd_{(CHUR)}0 = 0.512638$ and $^{147}Sm/^{144}Nd_{(CHUR)}0 = 0.1967$]. The ε_{NdT} values were calculated using the equation $\varepsilon_{NdT} = \varepsilon_{Nd(0)} - Q_{Nd} f_{Sm/Nd} T$, with the $_{(CHUR)}0$ values above and $Q_{Nd} = 25.09$. Table 7 presents the calculated ε_{HfT} values for these 24 samples, converted of the ε_{NdT} data using the Vervoort et al. (2011) equation. Extrapolation allows comparing published data (Ribeiro et al., 2020). – see Table 7.

4. Results

Most documented U–Pb zircon age determinations in the Bolivian Precambrian Shield were carried out on granitic units. More data should be referred to the country rocks, e.g., LMGC, CGC, and SISG, implying that their ages still need to be better constrained. Age results are listed in Table 6. Figs. 2 and 3 present the results for our samples.

4.1. *U–Pb results*

4.1.1. *San Ignacio schist group*

4.1.1.1. Ambaybo rhyolite. A rhyolite (AD1402) was collected at Guapomo Hill (Adamek et al., 1996). It crops out on the upper part of the metavolcanic sedimentary sequence that belongs to the SISG in the San Ramon district -see Figs. 2 and 4a; Section 2.2 (Litherland et al., 1986;

Table 6
U–Pb SHRIMP analytical data for the studied samples.

Sample	*Ambaybo*															
	Ratio						err corr	%Com	Age (Ma)					ppm		Th/U
	$^{207}Pb/^{235}U$	err %	$^{206}Pb/^{238}U$	err %	$^{207}Pb/^{206}Pb$	err %		^{206}Pb	$^{206}Pb/^{238}U$	1 α	$^{207}Pb/^{206}Pb$	1 α	Disc %	U	Th	
13.1	4.0	3.4	0.29	2.0	0.102	2.7	0.9	48	1626	28	1659	51	2	194	97	0.51
16.1	4.3	4.1	0.29	1.9	0.106	3.6	0.6	41	1652	27	1725	66	5	164	76	0.48
12.1	4.3	4.7	0.29	1.9	0.106	4.2	0.7	21	1653	28	1725	78	5	83	55	0.69
17.1	4.3	2.7	0.29	1.8	0.106	2.0	0.8	41	1661	26	1724	36	4	164	76	0.48
8.1	4.2	3.6	0.29	1.9	0.105	3.1	0.7	26	1661	27	1709	57	3	105	38	0.37
11.1	4.2	3.2	0.29	1.8	0.103	2.7	0.9	39	1660	27	1681	49	1	156	91	0.60
10.1	4.2	2.2	0.29	1.8	0.102	1.4	0.9	55	1664	26	1666	25	0	216	119	0.57
1.1	4.2	2.9	0.30	1.8	0.102	2.3	0.9	47	1672	26	1666	42	0	184	104	0.59
14.1	4.2	2.0	0.30	1.8	0.103	0.8	0.6	56	1678	26	1686	15	1	218	115	0.55
18.1	4.5	2.4	0.30	1.8	0.109	1.6	0.6	42	1689	27	1787	29	6	164	87	0.55
15.1	4.3	3.3	0.30	1.8	0.105	2.8	0.8	48	1686	27	1709	51	2	189	104	0.57
2.1	4.2	2.9	0.30	1.8	0.103	2.2	0.7	33	1687	27	1679	41	−1	129	61	0.49
3.1	4.4	2.1	0.30	1.8	0.105	1.2	0.5	66	1697	26	1720	22	2	257	132	0.53
7.1	4.3	2.0	0.30	1.8	0.104	0.8	0.7	49	1696	27	1699	15	0	190	114	0.62
4.1	4.4	2.4	0.30	1.8	0.105	1.6	0.8	58	1699	27	1715	30	1	225	127	0.59
5.1	4.3	2.0	0.30	1.7	0.103	1.0	0.6	86	1706	26	1685	18	−1	331	184	0.57
19.1	4.3	1.9	0.30	1.8	0.104	0.7	0.6	45	1708	27	1691	13	−1	174	78	0.46
9.1	4.4	2.6	0.31	1.8	0.104	1.9	0.7	50	1716	27	1704	35	−1	192	105	0.56
6.1	4.4	1.8	0.31	1.7	0.104	0.5	0.7	99	1725	26	1703	9	−1	376	279	0.77

Sample	*La Cruz*															
	Ratio						err corr	%Com	Age (Ma)					ppm		Th/U
	$^{207}Pb/^{235}U$	err %	$^{206}Pb/^{238}U$	err %	$^{207}Pb/^{206}Pb$	err %		^{206}Pb	$^{206}Pb/^{238}U$	1 α	$^{207}Pb/^{206}Pb$	1 α	Disc %	U	Th	
pelc0558–1.1	3.841	2.1	0.2572	1.5	0.1083	1.4	0.728	3.02	1.475	23	1.692	65	13	244	160	0.68
pelc0558–2.1	1.045	2.2	0.0907	1.3	0.0836	1.8	0.605	2.16	559.4	8.2	1.618	49	65	932	240	0.27
pelc0558–3.1	4.157	1.8	0.2906	1.5	0.1037	1.1	0.807	0.34	1.645	23	1.656	27	1	257	136	0.55
pelc0558–4.1	1.590	1.7	0.1063	1.4	0.1085	1.0	0.795	4.16	651.3	9.8	1.741	57	62	1413	586	0.43
pelc0558–5.1	5.096	1.9	0.2903	1.5	0.1273	1.0	0.830	0.37	1.643	24	1.673	27	5	186	122	0.68
pelc0558–6.1	4.151	2.2	0.2968	1.6	0.1014	1.5	0.747	0.30	1.676	28	1.646	30	−2	138	123	0.92
pelc0558–7.1	4.458	1.9	0.3064	1.5	0.1055	1.1	0.808	0.27	1.723	24	1.691	29	−2	279	120	0.44
pelc0558–8.1	4.213	1.8	0.2899	1.5	0.1054	0.97	0.842	0.11	1.641	24	1.684	19	3	317	192	0.62

Sample	*San Martín*															
	Ratio						err corr	%Com	Age (Ma)					ppm		Th/U
	^{207}Pb	err	^{206}Pb	err	^{207}Pb	err		^{206}Pb	^{206}Pb	1 α	^{207}Pb	1 α	Disc %	U	Th	
sub-1.1	2.817	0.83	0.2398	0.47	0.08520	0.68	0.571	0.16	1.386.0	6	1.334	16	−4	976	41	0.04
sub-2.1	2.479	0.65	0.2094	0.45	0.08585	0.48	0.685	0.16	1.225.8	5	1.363	10	10	2782	61	0.02
sub-3.1	2.920	1.6	0.2484	0.77	0.0853	1.4	0.491	0.00	1.430	11	1.398	25	−3	247	100	0.42
sub-4.1	3.012	1.5	0.2521	0.75	0.0867	1.3	0.492	0.00	1.450	10	1.433	24	−2	260	94	0.37
sub-5.1	2.976	0.80	0.2474	0.47	0.08723	0.64	0.587	0.18	1.425.5	6.3	1.395	14	−2	1008	276	0.28
sub-6.1	2.576	1.4	0.2220	1.1	0.08417	0.88	0.792	0.19	1.292	14	1.301	19	1	1464	49	0.03
SUB-8.1	3.188	1.8	0.2778	0.85	0.0832	1.6	0.471	0.49	1.581	13	1.358	41	−17	163	54	0.34
SUB-8.1	3.095	1.5	0.2546	0.73	0.0881	1.3	0.483	0.09	1.462	10	1.399	25	−5	271	93	0.35
SUB-9.1	3.184	1.5	0.2682	0.82	0.0861	1.3	0.547	0.00	1.532	12	1.442	22	−7	259	117	0.47
SUB-10.1	2.705	1.8	0.2220	0.87	0.0884	1.6	0.480	0.00	1.293	11	1.428	30	9	218	51	0.24

Sample	*La Junta*															
	Ratio						err corr	%Com	Age (Ma)					ppm		Th/U
	^{207}Pb	err	^{206}Pb	err	^{207}Pb	err		^{206}Pb	^{206}Pb	1 α	^{207}Pb	1 α	Disc %	U	Th	
512.2	2.508	2.9	0.2157	2.4	0.0844	1.6	0.825	0.06	1.259	30	1.389	30	9	168	117	0.72
512.3	3.033	2.5	0.2480	2.3	0.0886	0.94	0.924	0.03	1.429	30	1.486	18	3	452	106	0.24
512.4	2.397	2.3	0.2023	2.2	0.0859	0.42	0.983	0.29	1.188	25	1.387	10	14	3134	190	0.06
512.5	2.651	2.7	0.2314	2.3	0.0831	1.3	0.866	0.04	1.342	30	1.368	25	1	259	127	0.51
512.6	1.831	5.3	0.1620	2.3	0.0820	4.8	0.431	4.08	970	23	1.339	120	27	542	101	0.19
512.7	2.595	2.6	0.2197	2.3	0.0857	1.2	0.881	0.28	1.280	28	1.332	27	4	442	78	0.18
512.8	2.443	3.0	0.2229	2.4	0.0795	1.8	0.796	0.63	1.298	32	1.398	45	6	176	131	0.77

Sample	*Diamantina*															
	Ratio						err corr	%Com	Age (Ma)					ppm		Th/U
	^{207}Pb	err	^{206}Pb	err	^{207}Pb	err		^{206}Pb	^{206}Pb	1 α	^{207}Pb	1 α	Disc %	U	Th	
3057–1	136	136	0.2445	0.66	0.08550	1.2	0.496	0.05	1410.0	8.9	0.08550	1.2	−3	332	136	136
3057–2	2452	2452	0.18909	0.40	0.05988	0.95	0.392	0.24	1118.2	6.4	0.05988	0.95	13	2377	2452	2452
3057–3.1	47	47	0.2127	0.54	0.08657	0.83	0.546	0.22	1243.3	6.2	0.08657	0.83	6	683	47	47
3057–3.2	212	212	0.22978	0.39	0.08648	0.45	0.654	0.62	1333.8	4.8	0.08648	0.45	2	2753	212	212

(*continued on next page*)

Table 6 (*continued*)

Sample	*Diamantina*															
	Ratio						err corr	%Com	Age (Ma)					ppm		Th/U
	^{207}Pb	err	^{206}Pb	err	^{207}Pb	err		^{206}Pb	^{206}Pb	1 α	^{207}Pb	1 α	Disc %	U	Th	
3057–5	104	104	0.2298	0.78	0.0859	1.5	0.464	0.31	1334	10	0.0859	1.5	5	274	104	104
3057–6	65	65	0.2276	1.1	0.0786	2.2	0.451	0.70	1323	15	0.0786	2.2	−3	140	65	65
Sample	*San Andrés*															
	Ratio						err corr	%Com	Age (Ma)					ppm		Th/U
	$^{207}Pb/^{235}U$	err %	$^{206}Pb/^{238}U$	err %	$^{207}Pb/^{206}Pb$	err %		^{206}Pb	$^{206}Pb/^{238}U$	1 α	$^{207}Pb/^{206}Pb$	1 α	Disc %	U	Th	
404.1	2.186	3.2	0.2055	2.5	0.0771	2.1	0.761	0.24	1.205	30	1.263	39	4	149	89	0.61
404.2	2.318	3.4	0.2046	2.5	0.0821	2.3	0.738	0.76	1.200	30	1.175	57	−2	98	60	0.63
404.3	2.257	2.6	0.2016	2.3	0.0812	1.2	0.879	1.08	1.184	26	1.194	47	1	434	101	0.24
404.4	2.102	3.9	0.1885	2.6	0.0809	2.8	0.683	0.16	1.114	30	1.357	54	17	79	45	0.59
404.5	2.201	2.6	0.2036	2.3	0.07841	1.2	0.884	0.00	1.195	27	1.298	22	7	413	240	0.60
404.6	2.368	3.1	0.2146	2.4	0.0800	1.9	0.783	–	1.253	29	1.348	34	6	130	54	0.42
404.7	2.213	2.9	0.2172	2.3	0.0739	1.8	0.799	0.00	1.268	31	1.286	30	0	192	158	0.85
404.8	2.033	3.8	0.2104	2.6	0.0701	2.8	0.680	0.00	1.232	32	1.269	45	2	92	57	0.64
404.9	2.149	3.5	0.2004	2.5	0.0778	2.4	0.726	0.27	1.178	30	1.279	45	7	110	75	0.70
404.1	2.520	2.7	0.2219	2.3	0.0824	1.3	0.868	0.08	1.292	29	1.308	26	1	293	126	0.44
404.11	2.288	3.1	0.2129	2.4	0.0779	2.0	0.765	0.21	1.245	29	1.261	41	1	144	73	0.53
404.12	2.332	2.9	0.2062	2.4	0.0820	1.7	0.808	0.19	1.209	30	1.289	38	6	175	143	0.85
404.13	3.487	2.5	0.2680	2.3	0.09436	1.0	0.910	0.12	1.531	34	1.616	18	5	318	205	0.67
404.14	1.756	2.9	0.1784	2.3	0.0714	1.7	0.812	0.20	1.059	25	1.285	29	16	312	153	0.51
404.13.2	2.226	2.9	0.2021	2.3	0.0799	1.7	0.810	0.34	1.187	27	1.317	41	9	242	111	0.48

Witschard et al., 1993; López-Montaño and y Bernasconi, 1988; Matos, 2010). The analyzed zircon grains are between 73 and 183 μm long. The U content is variable, of 83–376 ppm, while Th/U varies between 0.37 and 0.77. No grains are metamorphic (Table 6). All grains have distinct concentric growth zoning. The concentric growth is interpreted to represent zircon growth at the time of the emplacement of the rhyolite. Seventeen SHRIMP analyses regress to yield a weighted mean $^{207}Pb/^{206}Pb$ age of 1690.8 ± 8.1 Ma (MSWD = 4.5).

4.1.2. *Yarituses Suite*

Sample SR83 was collected at Santa Rosa farm, 8 km east of San Javier on the road to Talcoso hill (Fig. 2). This rock is a leucogranite, white in color, massive to weakly foliated. K-feldspar is microcline and subordinately appears orthoclase, while plagioclase tends to be euhedral. The mafic mineral is biotite scarcely distributed in the rock (<2%); the principal accessory is brown granular sphene. TIMS analyses of sample SR83 of four multigrain zircon fractions, three concordant plus one discordant analysis, yielded $^{207}Pb/^{206}Pb$ age of 1673 ± 25 Ma, and MSWD = 36 (Matos-Salinas, 2010).

The La Cruz syenogranite (sample 558) comprises two elongated bodies 6 and 8 km long. They show NNW-SSE orientation (Fletcher, 1979) and are tectonically controlled by shear zones (Adamek et al., 1996). The outcrops expose a homogeneous rock, medium-grained and light pink. K-feldspar is characterized by abundant flame-like or braided pattern perthite with scarce biotite as the mafic mineral; the dominant texture is allotriomorphic granular. This syenogranite is cut by numerous quartz veins and is moderately jointed. In parts, the intrusion is weakly foliated. Zircon grains of the La Cruz granite are between 100 and 220 μm long. The U content of zircon is variable from 138 to 932 ppm; only one analyzed grain contains 3134 ppm. The Th/U ratios vary between 0.27 and 0.92, suggesting a magmatic origin. The CL images show that most of the crystals are euhedral and have both parallel-faces zoning and distinct concentric growth (Fig. 4b). The SHRIMP analysis of eight zircon grains (Table 6), with two cores, lie on the Concordia with a weighted mean $^{207}Pb/^{206}Pb$ age of 1673 ± 21 Ma (MSWD = 0.67) (Fig. 4a), considered as the emplacement of the body.

4.1.3. *Pensamiento Granitoid Complex*

4.1.3.1. San Martín granite. This pluton (CA0509) is one of the most considerable syn-to late-kinematic intrusions of the PGC, and it crops out on the western side of the Paraguá Domain (Fig. 2). This weakly foliated granite has a granular appearance with biotite flakes and prismatic hornblende, containing K- feldspar phenocrysts of 1.5–3 cm long. In places, a lens or augen-texture is developed. On the western side of the batholith, the mineral assemblage reached medium metamorphic grade conditions. The analyzed zircon grains are commonly between 150 and 275 μm, mostly euhedral. The U content is a variable from 160 to 2700 ppm. The Th/U ratios are between 0.24 and 0.47, but three analyses showed Th/U ratios as low as 0.02–0.04. The most common zircon morphology shows oscillatory zoning in the (CL imagery). However, some grains present a moderately gray-CL core (Fig. 4b).

Ten analyses of morphologically different zircon grains of the two main populations were obtained (Table 6). Six magmatic cores yielded a$^{207}Pb/^{206}Pb$ age of 1409 ± 17 Ma (MSWD = 1.06). In contrast, three metamorphic rims yielded 1318 ± 14 Ma (MSWD = 1.4) (Fig. 4a). Given the concentrically zoned zircon grains of the igneous population, we interpret the upper intercept SHRIMP age as the emplacement time of the San Martín granite that later underwent a metamorphic episode.

4.1.3.2. La Junta granite. SHRIMP U–Pb data were performed for the La Junta Granite. Its sample (LJ0512) was collected along the road to Campamento (Fig. 2). Zircon grains from this sample are 165–235 μm and commonly show well-formed euhedral terminations. The CL images show crystals generally with cores with light gray oscillatory zoning, surrounded by thin mantles of low-CL zircon. The low-CL rims show subtle concentric zoning (Fig. 4b). Some grains are dark gray due to the high U content. Seven analyses of zircon grains were performed on this sample. The zircon cores are characterized by U concentrations of 168–542, but one grain exceptionally has 3154 ppm. The Th/U ratios vary between 0.18 and 0.77, whereas only one grain yields 0.06 (Table 6). Five core analyses regress to produce an upper intercept SHRIMP age of 1380 ± 17 Ma (MSWD = 0.84) (Fig. 4a) and constrain the emplacement age.

4.1.3.3. Diamantina granite. One syenogranite (CP0507) was collected

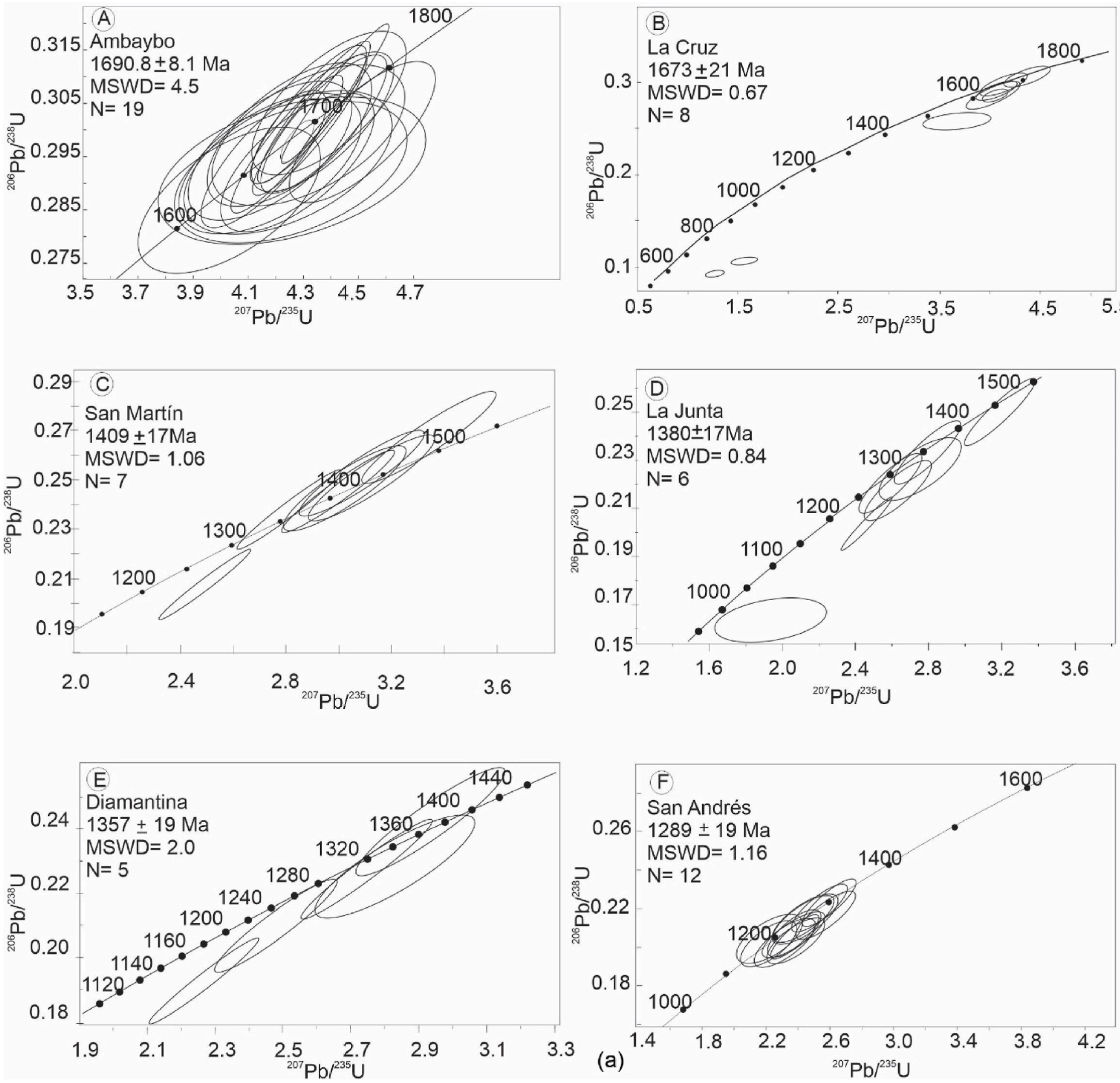

Fig. 4. (A) SHRIMP diagrams for studied rocks in the Paraguá Domain: A) Ambaybo rhyolite, B) La Cruz, C) San Martín, D) La Junta, E) Diamantina, and F) San Andrés granites. (b) Cathodoluminescence images of granite zircons of B–F), indicating the spot point dated by the SHRIMP.

at Cerro Pelado Hill (Fig. 2). The zircon grains are between 160 and 270 μm long. The U content varies from 140 to 683 ppm, while Th/U varies between 0.39 and 1.07. Two grains are metamorphic, containing U content of 2377 and 2753 ppm, respectively (Table 6). CL images show that all zircon grains have distinct concentric growth zoning, often truncated by overgrowth rims (not analyzed). Six analyses of five zircons yield a weighted mean $^{207}Pb/^{206}Pb$ age of 1357 ± 19 Ma (MSWD = 2.0) (Fig. 4a and b), representing zircon growth at the emplacement time of the granite.

4.1.3.4. San Andrés granite. We have sampled this intrusion (SA0404) at the Candelaria farm, 28 km SW of Concepción (Figs. 1 and 2). Zircon grains are clear and euhedral prismatic. The crystals range from 50 to 120 μm in length. The CL images reveal that most grains have oscillatory zoning, indicating magmatic origin (Fig. 4b). A total of 15 analyses were performed on 14 zircon grains of sample SA0404. They have U contents ranging from 79 to 434 ppm and Th/U of 0.24–0.85 (Table 6). The SHRIMP U/Pb data in twelve grains define an upper intercept $^{207}Pb/^{206}Pb$ age of 1289 ± 19, interpreted as a magmatic age (Fig. 4a). Furthermore, one analysis of an inherited age (grain 1.13) yields a $^{207}Pb/^{206}Pb$ age of 1616 ± 18 Ma (MSWD = 1.16). If true, this suggests protoliths like the Refugio granite of Yarituses Suite located 5 km to the west.

4.2. Sm–Nd results

4.2.1. LMGC

Five samples of the LMGC (514, 515, 518, 528, and 531) yield the oldest T_{DM} model age values, between 2.24 and 1.71 Ga. The ε_{NdT} values range from +3.0 to −5.3, indicating mantle-derived magmas variably contaminated with Paleoproterozoic crust (Tables 1 and 7).

4.2.2. Yarituses Suite

The Yarituses suite, represented by the La Cruz, Sujalito, and Refugio granitic samples, gave T_{DM} model ages of 1.92 to 1.77 Ga. The calculated values of ε_{NdT} of +2.1 and −0.8, respectively, suggest a mixed source derived from Orosirian protoliths.

4.2.3. PGC

The San Ignacio granites in the Concepcion Sheet (Fletcher, 1979),

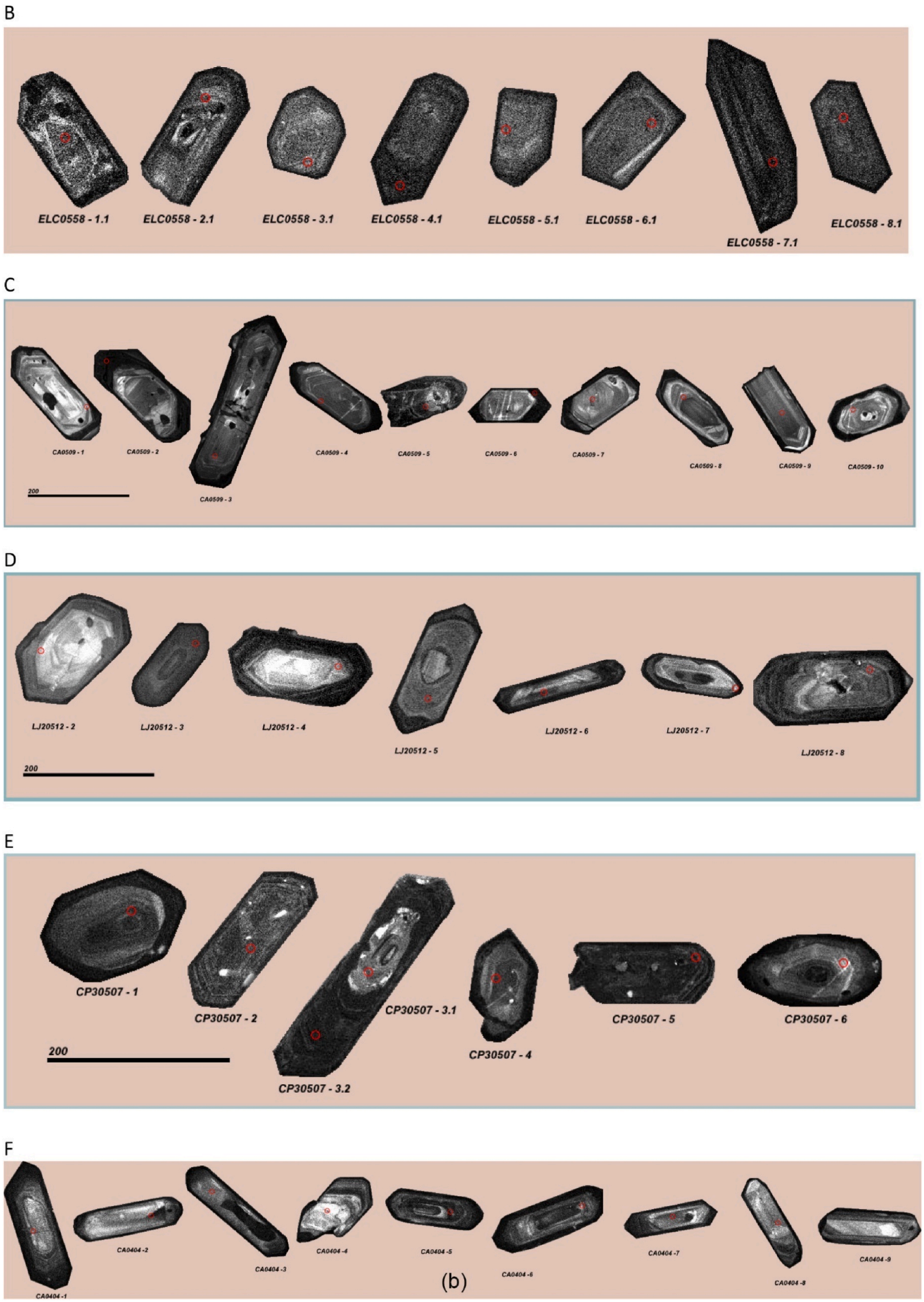

Fig. 4. (*continued*).

represented by the San Ramon, San Andres, San Javier, San Rafael, Limones, and Guarayos bodies, show T_{DM} model ages of 2.10–1.65 Ga (Tables 3 and 7) The ε_{NdT} values of +0.1 to −3.7 suggest a significant contribution of crustal components in the petrogenetic process. The granite rocks that crop out between Cerro León and San Antonio de Lomerío (Fig. 2, Table 7), represented by the El Carmen, Santa Rosario,

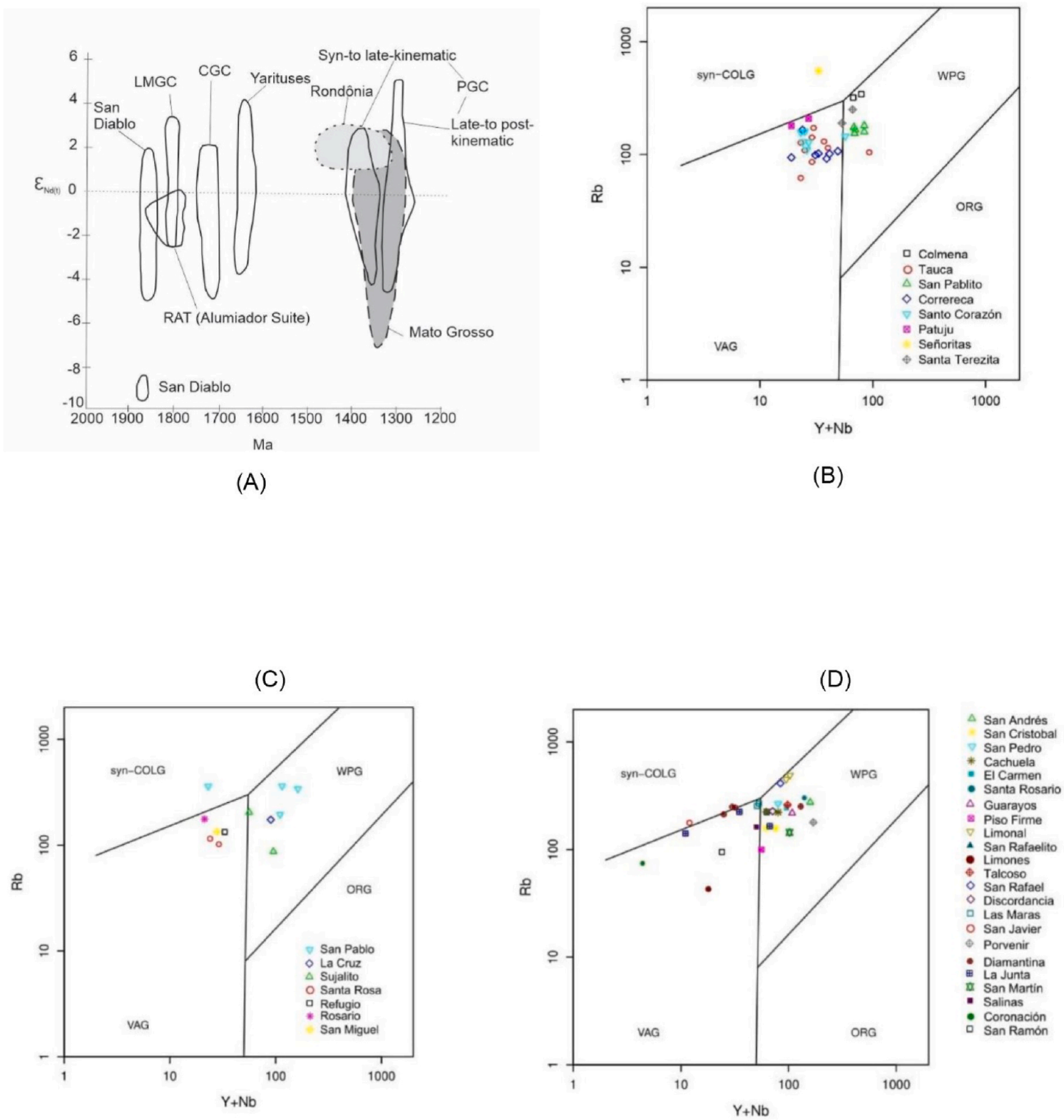

Fig. 5. A) Whole-rock Nd isotopic constraints for the San Ignacio granites of Pensamiento Granitoid Complex, and potential correlative tectonics units in Rondonia, Mato Grosso, and Rio Apa Terrane related to the Yarituses suite, Chiquitania Gneiss Complex, Lomas Maneches Granulite Complex, and the San Diablo domain. B) The trace element discrimination diagram to the San Diablo domain shows that the most granitoid rocks plot on the volcanic arc field. San Ignacio granites of the San Diablo domain plot on the within plate field. The geochemical data of Correreca, Santo Corazón, and Santa Terezita were presented by Redes et al. (2020). Geochemical data from the Colmena, Tauca, San Pablito, Patuju, and Señoritas are presented in Supplementary Table T1. C) Y + Nb vs Rb diagram of Yarituses Suite showing an evolution from subduction-related margin granites that straddles the within plate field. The Rosario and San Miguel data were described by Redes (2021). Geochemical analyses from Refugio, Santa Rosa, Sujalito, and La Cruz are shown in Supplementary Table T1. The San Pablo data by Vargas-Mattos (2010). D) Y + Nb vs Rb diagram of the Pensamiento Granitoide Complex. Most samples of syn-to-late kinematic granites are volcanic arc related, whereas most samples of late-to-post-kinematic granites plot on the within plate. Data of the Piso Firme, San Cristobal, Porvenir, Diamantina, San Martín y La Junta granites from Matos et al. (2009); data of the Limonal, Talcoso, and Cachuela granites from Vargas-Mattos et al. (2020). The San Ramon, San Javier, San Andrés, San Rafael, San Pedro, El Carmen, Santa Rosario, San Rafaelito, Las Maras, Guarayos, Discordancia, and Limones granites are presented in Supplementary Table T1. Salinas and Coronación (San Ramón) granites come from Nedel (2020).

San Pedro, Limonal, Coloradillo, Monterito, and San Rafaelito plutons, show T_{DM} range between 2.42 and 1.41 Ga and the ε_{NdT} values between +5.2 and −4.6. Therefore, mantle and crustal protoliths participated in the evolution of these bodies (Table 7).

5. Discussion

The new and compiled zircon U–Pb ages, isotopic constraints, and geological information provided new insights into the geodynamic evolution of the Bolivian Precambrian Shield distinguished in the San Diablo and Paraguá domains. The integrated interpretation indicates that three arc-type processes progressively formed the continental crust, now established at 1941–1849 Ma, 1690-1610 Ma, and 1430-1270 Ma, respectively. The two oldest events are the San Diablo Rocks and the Yarituses Suite. The first time they defined significant magmatism across the Precambrian Shield of Bolivia with correlatives in the

Table 7
Sm–Nd and Hf isotopic data for the Bolivian Precambrian rocks.

Sample	Unit	East	North	Sm (ppm)	Nd (ppm)	$^{147}Sm/^{144}Nd$	$^{143}Nd/^{144}Nd$	$\varepsilon_{(0)}$	T_{DM} (Ga)	$\varepsilon_{(T1)}$	εHf	Hf model age (Ga)
Paraguá Domain												
San Ignacio granites												
404	San Andrés	591,538	8,202,865	30.76	161.515	0.1152	0.51188	−14.9	1.8	−1.6	−1.3	1.80
535	El Carmen	608,143	8,186,921	19.1	126.586	0.0913	0.51203	−11.9	1.3	+5.2	+9.3	1.26
538	Santa Rosario	611,545	8,161,667	14.56	73.08	0.1205	0.51218	−8.99	1.4	+3.4	+6.5	1.41
403	San Javier	554,034	8,100,387	1.988	15.764	0.0763	0.51152	−21.8	1.7	−1.3	−0.8	1.69
406	San Rafael	745,786	8,152,306	12.77	63.763	0.1211	0.51179	−16.6	2.1	−3.7	−4.6	2.10
412	San Pedro	580,114	8,156,767	8.71	34.059	0.1547	0.51211	−10.3	2.4	−4.6	−5.9	2.42
540	Coloradillo	618,959	8,151,123	17.84	91.03	0.1185	0.51187	−14.9	1.9	−1.7	−1.4	1.87
543	Limonal	629,430	8,142,042	10.51	49.3	0.1289	0.51198	−12.9	1.9	−1.4	−1.3	1.90
545	Monterito	609,480	8,152,641	17.93	94.91	0.1143	0.51188	−14.6	1.9	−0.6	+0.2	1.77
546	San Rafaelito	591,975	8,160,598	7.66	39.523	0.1172	0.51193	−13.9	1.8	−0.4	+0.6	1.76
549	Limones	535,349	8,180,169	7.87	74.163	0.0642	0.51142	−23.8	1.7	−1.2	−0.7	1.65
552	Guarayos	478,345	8,243,122	12.33	63.241	0.1179	0.51195	−13.4	1.7	+0.1	+1.3	1.73
401	San Ramón	552,489	8,262,872	7.65	53.742	0.0861	0.51159	−20.5	1.7	−0.3	+0.8	1.73
Yarituses Suite												
547	Sujalito	568,433	8,160,690	15.69	86.354	0.1099	0.51184	−15.6	1.8	−0.8	−0.1	1.77
558	La Cruz	564,815	8,172,721	11.39	60.583	0.1137	0.51184	−11.6	1.8	+2.1	+4.5	1.83
408	Refugio	569,780	8,200,723	2.81	17.014	0.1000	0.51161	−20.0	1.9	+0.2	+1.5	1.92
[a]SM-08	San Miguel			4.71	27.48	0.1036	0.51059	−18.1	1.8	+1.9	+0.3 & +6.9	2.3 & 1.9
[a]LR-19	Rosario			6.05	31.37	0.1165	0.51054	−16.3	1.9	+0.9	−0.9 & +8.9	2.3 & 1.8
Chiquitania Gneiss Complex												
532	Victoria	598,307	8,247,676	16.87	91.041	0.1121	0.51178	−16.7	1.9	−2.3	−2.3	1.88
551	Momené	492,607	8,223,228	21.85	96.481	0.137	0.5122	−8.54	1.7	+1.6	+3.7	1.67
Lomas Maneches Granulite Complex												
514	La Chontita1	661,421	8,297,922	17.13	111.629	0.0928	0.51158	−20.5	1.8	−2.9	−3.2	1.83
515	La Chontita2	661,080	8,294,234	7.03	36.48	0.1166	0.51162	−19.8	2.2	−2.8	−3.2	2.24
518	Rio Negro	574,116	8,298,963	17.15	100.626	0.1031	0.5118	−16.3	1.7	−0.4	+0.6	1.71
528	San Luis	588,374	8,275,158	0.54	4.087	0.0801	0.51152	−21.8	1.7	+3.0	+5.8	1.73
531	San Pastor	599,344	82,555,173	3.11	17.046	0.1105	0.51177	−17	1.9	+1.3	+3.2	1.88
San Diablo Domain												
516	Señoritas	214,362	8,080,743	3.51	20.68	0.1027	0.51153	−21.6	2.08	−5.3	−6.9	2.08

[a] San Miguel and Rosario granites from Redes (2021).

Paleoproterozoic provinces within SW Amazonia and the RAT. The youngest magmatism allows a relationship with the Alto Guaporé accretionary-collisional orogeny. Moreover, compiled data from Litherland et al. (1986) indicate that much younger mafic and felsic activity (1170-1000 Ma) associated with crustal shortening and tectonic reactivations, including isotopic resetting of Rb–Sr and K–Ar dates, are widespread. They are markers of the Sunsás orogeny that consolidated the continental crust of the SW portion of the Amazonian Craton (Teixeira et al., 2010; Nedel et al., 2020; Redes et al., 2020; Ribeiro et al., 2020, 2022a, 2022b).

Table 8 outlines the main geologic units, their ages, and the interpreted tectonic scenario of the Bolivian Precambrian Shield during the Paleo and Mesoproterozoic history. The integrated evolution is discussed based on the updated geologic information, ages, and isotopic

Table 8
Summary of the main geological units and tectonic setting of the Precambrian shield of Bolivia. See Fig. 1 for details.

	Tectonic event	Geological unit	Lithology	Tectonic environments
Paraguá Domain	Sunsás orogeny 1.2–1.0 Ga	Sunsás and Vibosi Groups, granites, and mafic-ultramafic bodies (1.11 Ga)	Arkoses, sandstone, schist, conglomerates. Dunites, norites, granophyre. Syn-to-late-kinematic and late-to-post-kinematic granites	Continental Andean-type arc
	San Ignacio/Alto Guaporé orogeny 1.4–1.28 Ga	Pensamiento Granitoid Suite 1.44–1.27 Ga	Intrusive into the LMGC, CGC, and the SISG. Pre, syn-to late-kinematic and late-to post-kinematic granites	Continental Andean-type magmatic arc
		Yarituses Suite 1.68–1.62 Ga	Granite bodies La Cruz, Refugio, and San Pablo (San Ramón area)	Accretionary arc
		Lomas Maneches suite 1.69–1.66 Ga	Granitic sills, bluish gray, medium-grained with biotite or hornblende	Accretionary arc
		SISG 1.69 Ga	Metapsamites, schists, phyllites, slates, mafic metatuffs, BIF, metachert, and metalavas of tholeiitic and felsic composition. Green schist facies	Ocean-floor setting
		CGC 1.69 Ga	Pale pink to gray biotite gneiss and banded, micaceous quartz-feldspathic gneisses of amphibolite facies	Convergent intra-arc
		LMGC 1.82 Ga	Massive poorly banded or poorly foliated granulite rock intercalated with gneisses. Bands of charnockític, enderbitic and basic hypersthene bearing rocks that contain hypersthene or cordierite	Collision-related
San Diablo Domain		Correreca, Santo Corazon, Tauca, Santa Terezita gneisses 1.87–1.84 Ga	Quartz-feldspathic granites, fine to coarse-grained with biotite	Volcanic arc
		Las Tojas gneiss 1.94 Ga	Gray medium-to coarse-grained gneiss. Streaky banded biotite-muscovite and augen gneiss.	–

constraints. The potential relationships with the recognized tectonic-magmatic events that constructed the SW portion of the Amazonian Craton, including the distal RAT, are also addressed using the isotopic signatures as a case.

5.1. 1941–1849 ma event

This is the earliest magmatic event documented in the Bolivian Precambrian Shield, during which the San Diablo Domain was generated. The zircon Hf and coupled Nd isotopic evidence suggest the country rocks derived from moderately juvenile melts with significant input of recycled model age components as old as 2.7–2.0 Ga (see Table 7). The San Diablo crust results from an evolved accretionary arc, represented by the predominantly calc-alkaline to alkaline rocks (Redes et al., 2020). At a regional scale, the San Diablo crust is roughly coeval with rocks of the Western Domain of the RAT, as well as with a basement inlier far north in the Juruena crust and the country rocks in adjoining Ventuari-Tapajós Province (Fig. 1) (e.g., Teixeira et al., 2020 and references therein). Indeed, the idea of a petrogenetic link between the RAT, Paraguá Terrane, and Amazonia was already addressed by several works based on zircon U–Pb–Hf isotopic data (e.g., Ribeiro et al., 2020, 2022a, 2022b). According to the most reliable model, the Western Domain (2100-1840 Ma) of the RAT, the San Diablo Domain, and the Ventuari-Tapajós Province may represent reworking crustal magmatism produced by an advancing episode of the accretionary orogen in the Paleoproterozoic Amazonia.

5.2. 1690-1620 ma event

The 1690-1620 Ma tectonic-magmatic event produced significant crustal segments within the Paraguá Domain. Such an episode remobilized the crystalline basement (LMGC), represented by granulites and gneisses (1818 ± 13 Ma) with protoliths, as suggested by the negative (−3.8) and positive (+4.1) ε_{NdT} values (see Tables 1 and 8) demonstrating mixing of crustal and mantle components.

Four lithostratigraphic units formed during the 1690-1620 Ma event: the Chiquitania (CGC) ortho- and para-derived rocks, the San Ignacio metavolcanic-sedimentary units (SISG), and the roughly coeval granitoid intrusions (Yarituses and Lomas Maneches granitoid suites). The Yarituses Suite focused here comprises several plutons such as the La Cruz, Refugio, San Pablo, Sujalito, San Miguel, and Rosario granitoid intrusions, formed between 1683 and 1610 Ma, and represents the timing of significant crustal thickening that includes the granitic sills referred to as the Lomas Meneches Suite, previously documented by Boger et al. (2005). The San Miguel and Rosario granites (Fig. 2 and Table 7) show Paleoproterozoic Hf model ages (up to 2.3) and ε_{HfT} values as high as +8.9, indicating a derivation of a mantle source predominantly, in agreement with the positive ε_{NdT} parameters (Redes, 2021) – see Section 1.

The Yarituses Suite and the Chiquitania orthogneisses exhibit characteristic juvenile-like Nd isotopic signatures (Table 1) consistent with their derivation in an accretionary arc setting with some contribution of short-lived components (up to 1.7 Ga). This finding agrees well with the peculiar lithologies of the SISG (metapsamites, schists, phyllites, slates, mafic metatuffs, BIF, metachert, and metalavas of tholeiitic and felsic composition). In this context, the Ambaybo rhyolite may have originated in a back-arc setting akin to the continental arc hypothesized here.

At a regional approach, the 1690-1620 Ma episode has an age match with a granulite facies, partial melting episode (1.69–1.61 Ga), documented over the Jamari Terrane (Fig. 1), as is the Rondonia-San Ignacio Province (Bettencourt et al., 2010). According to Scandolara et al. (2017), this episode is marked by regional compressional and foliation features and thrusts – see Section 1. This fact agrees well with the onset of a continental arc with tectonic features overprinting the already stable foreland.

5.3. 1430-1340 ma event

The new and compiled U–Pb datings are used for achieving the tectonic significance of the San Ignacio orogeny in Bolivia. Table 3 describes the general characteristics of the main bodies of the PGC. We address the timing of the emplacement of the San Ignacio granitoid relative to the regional folding and coupled field relationships exemplified by intrusive aplites, pegmatite injections, and hornfels (Fig. 2). Collisional-type granulite facies metamorphism is apparent in a few outcrops (see details in Section 2). At the western border of the shield, around San Ramón, and on the west side of Talcoso Hill, the subvolcanic rocks are interpreted as the epizone of the granites.

This magmatic event, known in Bolivia as the PGC, is widespread over the Paraguá and San Diablo domains (Fig. 1). By extrapolation, we can invoke that juxtaposition of such distinct terranes occurred during the San Ignacio orogeny. Field information determined that this magmatism formed various felsic and mafic rocks with correlative analogs in the Brazilian counterpart. Such granitoid rocks are markers of the development of the Alto Guaporé orogeny, involving magmatic-arc convergence, ocean closure, and a continental collision of the intervening Paraguá Terrane against the active margin of the Rio Negro-Juruena province (e.g., Bettencourt et al., 2010; Rizzotto et al., 2014; Ribeiro et al., 2020, 2022a, 2022b). Indeed, the Nd isotopic and coupled geochemical evidence shows that this orogeny evolved in a magmatic arc setting (Bettencourt et al., 2010; Matos et al., 2009). During this event, the zircon metamorphic rims (1340–1320) record a medium-to high-grade metamorphism in the Paraguá Terrane.

The PGC new and compiled U–Pb data document crust formation between 1.45–1.34 Ga (syn-to late-kinematic plutons) and 1.33–1.27 Ga (late-to post-kinematic). The San Ramón granodiorite is interpreted as a pre-kinematic body (Fig. 3), suggesting that it refers to earlier stages of continental plutonism. In petrogenetic terms, the San Martin granite yielded an ε_{NdT} value of +1.8, whereas the La Junta granite shows a contrasting nature given by negative values down to −4.3 (Table 3). Also, the Diamantina granite has variable ε_{NdT} values (slightly positive and negative ones), characteristic of a crustal mixing nature (see Table 3), consistent with a continental arc setting. It is intrusive into the syn-to late-kinematic granites (La Junta, San Martin), suggesting it could be a late-to post-kinematic pluton. Its age correlates well with the several plutons in the Brazilian counterpart, such as the Alto Candeias, Ouro Fino, Fronteira, and Morrinhos plutons (Tables 3 and 4).

During the convergent-margin process of the Alto Guaporé orogeny, the inboard intraplate activity took place in the active continental margin of the proto-Amazonian Craton (Brazil), such as the Salto do Céu sills (1.44 Ga) and the Nova Lacerda dike swarm (1.39 Ga) (Teixeira et al., 2015b). In the Bolivian territory, the Coronación and San Ramón granodiorites of the locally known San Ignacio orogeny may be correlative with plutons assigned to the 1.48–1.42 Ga Santa Helena orogeny in the Jauru Terrane (Geraldes et al., 2001) as part of the Rondonian-San Ignacio Province (Fig. 1).

5.4. Isotopic inferences

The available Nd and Hf isotopic values of samples in the Bolivian Precambrian Shield are shown in Tables 1 and 2, respectively, and 7. Fig. 5a exhibits the Nd isotopic fields for the selected rocks referred to distinct tectonic domains recognized in the SW Amazonian Craton and RAT. In contrast, Fig. 5 b,c, and d present an integration of the compiled geochemical data. The integrated data provide the following inferences:

First, the ε_{NdT} compositional fields of the San Diablo Domain are distinct from that of the Paraguá Domain, given by a narrower spread for the $\varepsilon_{NdT,}$ besides some values as low as −9. Most values vary between −6.5 and +1.8, demonstrating the mixing of crustal and mantle components as old as 2.29 to 1.69 Ga (Table 1). The PGC rock in the San Diablo Domain of 6 samples yielded variable ε_{NdT} values as low as −6.5, implying they could result from crustal melts. Second, the rocks of the

Paraguá Domain, exemplified by the LMGC, the CGC, and the Yarituses Suite - T_{DM} model ages of 2.48 to 1.67 Ga show a more extensive range of the ε_{NdT} values of −4.9 to +4.1, reinforcing the distinct nature again compared to the San Diablo Domain – interpreted as a nearby crustal segment at the time (Table 1). The PGC continental arc in the Paraguá Domain produced voluminous plutonism with subordinate subvolcanic activity. These rocks have Nd T_{DM} model ages between 2.42 and 1.58 Ga and positive and negative ε_{NdT} values from +5.2 to −4.6 compatible at least with the melting of distinct crustal components but akin to the Paraguá Domain (Table 3; Fig. 5a). The Alto Guaporé magmatism portrays a roughly similar tectonic context (e.g., Bettencourt et al., 2010). All these results - e.g., San Diablo and Paragua domains-suggest magma sources akin to Paleoproterozic short-lived protoliths in a series of arc settings, supported by the calc-alkaline character of rocks and the volcanic arc diagram discrimination. The petrogenetic nature of the recognized units in the Precambrian Shield of Bolivia is explored below. Note, in Fig. 5a, the RAT field, represented by crustal-recycled rocks, fits mainly the LMGC field and partly the San Diablo one, indicating, therefore, the isotopic affinity (compiled data of Faleiros et al., 2016; Teixeira et al., 2020; Ribeiro et al., 2020, 2022a,b).

The tectonic discrimination diagram (Fig. 5b) for the San Diablo Domain shows that most samples plotted in the field are associated with continental arc magmatism and straddle the WPG. In particular, the plot of the ca. 1.45 Ga Señoritas sample (PGC) fits the syn-COLG field. It could be considered a pre-kinematic granite. The tectonic discrimination diagram of Fig. 5c belongs to the Yarituses Suite. It shows a dominant subduction field that classifies the rocks as originating in a continental arc environment, agreeing with the isotopic inferences. Few samples transgress into the WPG field. The geochemical discrimination diagram of the PGC rocks (Fig. 5d), the most representative intrusive suite on the Paraguá Domain (San Ignacio/Alto Guaporé orogen), shows syn-to late-kinematic signatures associated thus with subduction-related rocks. Most late-to post-kinematic granite samples transgress the magmatic arc's boundaries to the WPG. Since the syn-to late-kinematic granites show arc affinity and the late-to post-kinematic granites plot in the field associated with the within plate, it suggests peculiar features of both showing migration of the magmatic arc of NNE of the Paragua Domain to the SSW, e.g., of the Alto Guaporé belt to the San Ignacio belt. This crustal growth reflects a derivation of source rocks and tectonic regimes during the progressive development of convergent-to-collisional dynamics during which the RAT and the Paraguá Terrane (Paraguá/San Diablo) were docked to the SW Amazonian Craton as it is reflected in the Nd signature (e.g., Ribeiro et al., 2020, 2022a; and b).

Fig. 6a shows the ε_{HfT} data of the Paraguá Domain (LMGC, CGC, Yarituses Suite, and the PGC), converted by the recalculation of the available ε_{NdT} data using the Vervoort et al. (2011) equation (Table 7), for further petrogenetic inferences. The ε_{HfT} data shows a gradual course of subchondritic sources toward suprachondritic sources throughout time, comparing well with the isotopic features documented by Ribeiro et al. (2022b). For instance, the LMGC data form an array of moderate slopes of ε_{NdT} of −6.9 to +5.8 and Hf model ages between 2.24 and 1.71 Ga, which evolved through a time of a juvenile source to crustal remobilization. Similarly, the Yarituses suite defines an ε_{HfT} time array showing values of −2.6 to +4.5 and the Hf model ages of 2.48 to 1.77 Ga. Such source rocks involved in the generation of this suite might be juvenile material and a contribution of older crust in the magma sources.

However, we know that such a speculation is based on whole rock Hf data extrapolated from the Nd ones. At the same time, PGC samples delineate a slope-lying trend characterized by highly variable ages of 2.42 to 1.41 Ga and ε_{HfT} values of −5.9 to +9.3. Therefore we infer that distinct and more extensive sources must have contributed to generating such plutonism as expected in a continental arc setting. Fig. 6b presents an integrated plot of the εHfT and the crystallization ages of the RAT compared to the San Diablo and Paraguá domains, in conjunction with a compilation of igneous and detrital zircons related to the SW Amazonian Craton supporting the previous correlation of Ribeiro et al. (2020;

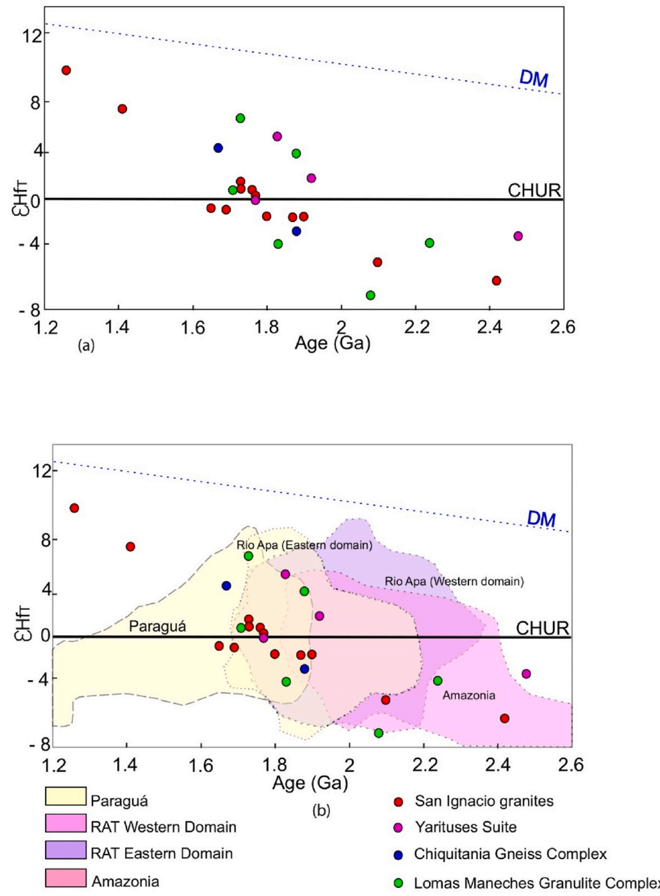

Fig. 6. A) ε_{HfT} data vs age of Paraguá domain, Lomas Maneches Granulite Complex, green; Chiquitania Gneiss Complex, blue; Yarituses Suite, pink and the Pensamiento Granitoid Complex, red) converted of ε_{NdT} data using Vervoort et al. (2011) equation. b) ε_{HfT} data vs age of Paraguá domain, compared to samples of the Rio Apa Terrane, Paraguá, and Amazonia following Ribeiro et al., 2022a,b. References to color in this figure legend as A).

Fig. 9). Fig. 6b shows that LMGC, the Yarituses Suite, and the PGC share with APAwestern and Eastern domains between 1950 and 1700 Ma and ε_{HfT} between −4 and +6, suggesting a petrogenetic link. The two samples on the left corner (Fig. 6a) belong to the San Ignacio granites south of Concepción town (Fig. 2). It shows values nearest T_{DM}. Additionally, it records the youngest age between 1.26 and 1.41.

5.5. The bolivian Precambrian Shield and growing Proterozoic Amazonia

Fig. 7 shows the time-correlation tectonic chart for the San Diablo and Paraguá domains, allowing inferences that three distinct tectonic-magmatic events built the continental crust of the Orosirian to the Ectasian. The vertical arrows indicating the ancestry of the continental crust inferred from Nd isotopic data for representative units are also shown, pointing to protoliths as old as 2.1–2.3 Ga in both the San Diablo and Paraguá domains. Conversely, vertical bars in blue represent the values of the Hf model ages (Ga) converted by the recalculation of the ε_{NdT} data using the Vervoort et al. (2011) equation (See Table 7) and showing similar characteristics.

The earliest accretionary episode formed the San Diablo Domain, represented by the Las Tojas gneiss, associated with crustal thickness under medium-grade metamorphism (e.g., Correreca and other rocks). Both episodes may represent a single accretionary phase contemporaneous to the time of formation of Western terrane RAT –proof of their tectonic affinity also supported by Hf–Nd isotopic constraints (see above). We note that the basement of the Paraguá Domain is slightly

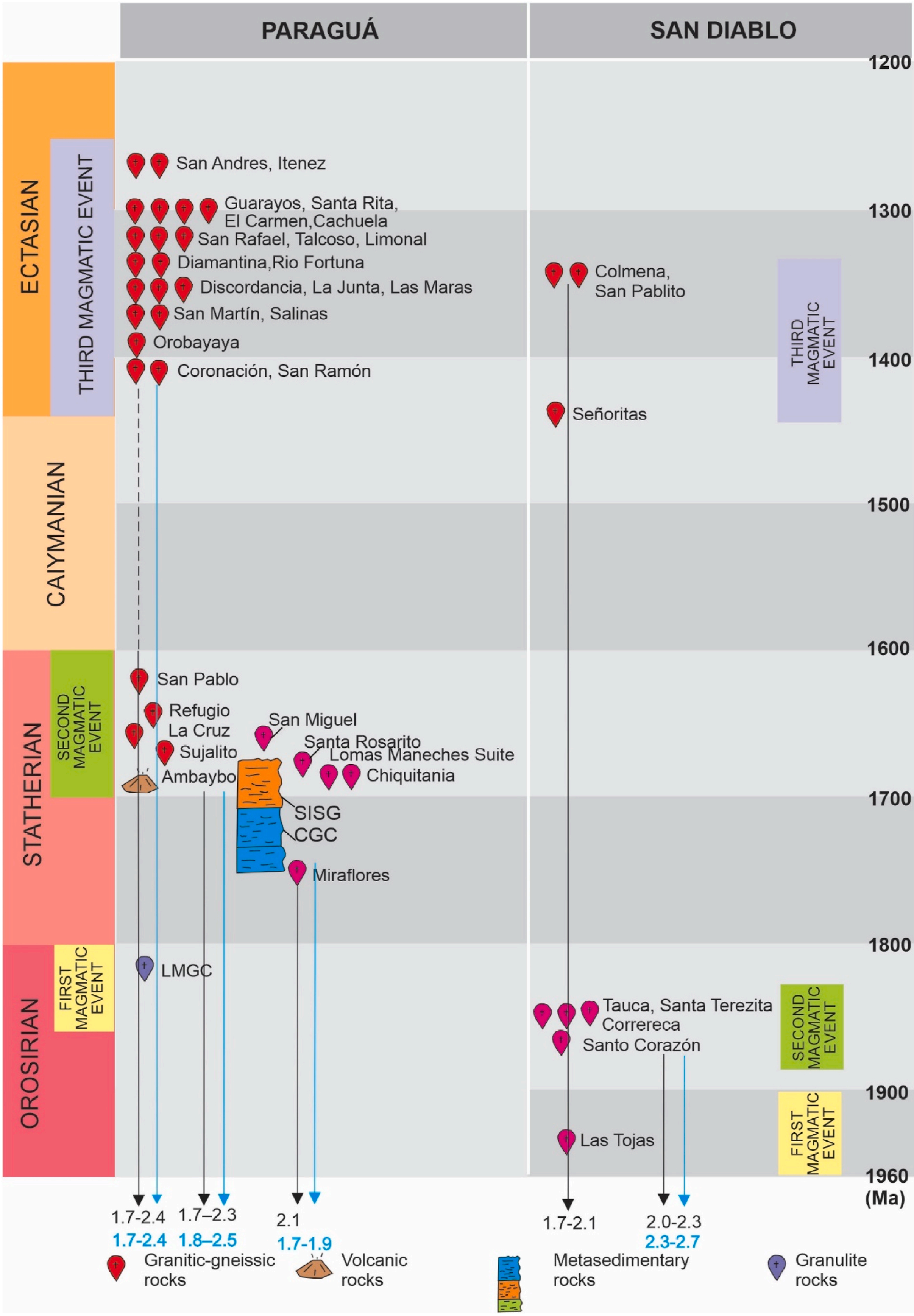

Fig. 7. Time-correlation tectonic chart for the San Diablo and Paraguá domains of the Paleo-to Mesoproterozoic time of the Bolivian Precambrian Shield (adapted of Teixeira et al., 2019a). Vertical bars in black show the range of the Sm–Nd T_{DM} ages (Ga). Vertical bars in blue display the range of the Hf model ages (Ga).

younger than the crustal thickening of the San Diablo crust (i.e., LMGC), implying that each domain has undergone a particular and separated evolution in time and space. The Paraguá Domain hosts additional evidence for such a hypothesis: the record of a specific younger accretionary episode, given by plutons and sills of the Yarituses and Lomas Maneches granitoid suites, and the roughly coeval CGC and SISG units altogether generated in a continental arc evolved in early Statherian (ca. 1.65 Ga).

The San Diablo and Paraguá domains experienced a third major accretionary/collisional episode which is tectonically related to the Guaporé orogeny (see above), developed in the Ectasian. Fig. 7 shows that the entire San Ignacio granites like San Martín, la Junta, Diamantina, Talcoso, Guarayos, etc., of the Paraguá Domain, share ages and Nd isotopic similarities with the Señoritas, Colmena, San Pablito granites of the San Diablo Domain. Additionally, the Colmena and San Pablito granites of the San Diablo Domain produced U–Pb zircon ages similar to most units of PGC, granite rocks of Mato Grosso and Rondonia suggesting that they belong to the same evolutionary history. Additionally, the Señoritas granite of the San Diablo Domain could be correlated with Coronación and San Ramón of the Paraguá Domain and Rio Piolho and Praia Alta of Rondonia.

Following Rizzotto and Hartmann (2012), the Alto Guaporé orogeny produced an arcuate belt covering an area of 95 km extended and 20 km wide of SE of Rondonia to the SW of Mato Grosso (see Fig. 1). The ophiolite remnants (1.47–1.43 Ga) indicate an intraoceanic arc setting evolved toward an oceanic closure along the Guaporé suture zone due to plate convergence. There is a consensus in the literature that the Paraguá Terrane accreted against the proto-Amazonian Craton at ca. 1.35–1.34 Ga (Bettencourt et al., 2010; Rizzotto et al., 2013; Ribeiro et al., 2020, 2022a, 2022b). Noteworthy, the U–Pb analyses of the 1.66 Ga granitoid sills (Boger et al., 2005) contain zircon rims that yielded an age of 1.32 Ga, interpreted as the time of partial melting, reinforcing the idea of the juxtaposition of the Paraguá Terrane along the continental margin of Amazonia. These findings support the critical role of “San Ignacio” overprints across the Bolivian Precambrian Shield, as suggested by some Rb–Sr and K–Ar dates on the PGC (Table 1). Late-to post--kinematic intrusions dated at 1.27 Ga (e.g., San Andres) indicate the orogenic collapse.

Likewise, the Bolivian Precambrian shield, the Brazilian counterpart, hosts pieces of evidence of such an essential accretionary episode (Bettencourt et al., 2010; Rizzotto and Hartmann, 2012; Rizzotto et al., 2013): for instance, A-type and rapakivi intrusive suites (1.35–1.31 Ga) such as the Alto Candeias and São Lourenço-Caripunas units (Table 4). In a similar manner, around Costa Marques (Fig. 2) along the boundary between Rondônia (Brazil) and Beni (Bolivia), granites, quartz syenites, trachytes, and rhyolites collectively ascribed to the Ouro Fino Suite yielded U–Pb ages of ca. 1.35 Ga, allowing a relationship with the Alto Guaporé orogen. The zircon Hf isotope signatures (+0.1 to +2.9) indicate that these rocks derived from juvenile accretion episodes (Bettencourt et al., 2014; Leite et al., 2016), whereas the positive ε_{NdT} values of +1.0 to +2.8 are consistent with a mantle derivation of these rocks. In the state of Mato Grosso, there is roughly coeval magmatic activity (1.41–1.28 Ga) (e.g., Lajes and Tarumã granites Cascata, Passagem, Fronteira, Guaporeí, and Morrinhos plutons) – Table 5 – showing calc-alkaline character and ε_{NdT} values (of −7 to +3.4) indicative of their nature due to crustal mixing (Fig. 5a).

Finally, the potential correlation between the Bolivian Precambrian Shield and Ectasian Amazonia is outstanding by several features related to the Sunsás collisional orogeny, see Teixeira et al. (2010). Note that intraplate magmatism correlates well with the onset of the Sunsás belt, exemplified by the 1.11 Ga Huanchaca-Rincón del Tigre LIP event (the Rincón del Tigre complex, the Huanchaca sills, and dikes in the Paraguá and San Diablo domains). This age matches the Rio Perdido dike swarm in the RAT (Fig. 1). From a paleogeográfic perspective, all these terranes were neighbors during the Sunsás orogeny (Teixeira et al., 2019a).

6. Tectonic model

As the available geological-isotopic knowledge suggests, Fig. 8 outlines the stepwise Proterozoic tectonic evolution of the Bolivian Precambrian Shield. We recognize two domains: San Diablo on the South and Paraguá on the North. At the San Diablo Domain, the Las Tojas gneiss was intruded on by the Correreca, Santo Corazon, Tauca, and Santa Terezita plutons; Fig. 8a (Faleiros et al., 2016; Teixeira et al., 2020; Ribeiro et al., 2020, 2022a, 2022b).

The most crucial event in the Paraguá Domain, which lasted from 1680 to 1610 Ma, was ascribed to the Yarituses suite, exemplified by the several plutons produced in an active continental margin setting (Fig. 8b). After a ca. 150 Ma quiescence of the continental crust, an Island Arc System (IAT) occurred at about 1470 Ma leading to juvenile ultramafic and mafic rocks, resuming the Alto Guaporé orogeny (1470 -1430 Ma) (Fig. 8c). This orogeny occurred as a result of the collision of the island arc (IAT) against Amazonia (Fig. 8d). The accretionary phase with ophiolite remnants, oceanic basalts, and island arc tholeiites akin to new subduction beneath the oceanic lithosphere between the Amazonia and the Paraguá Terrane, accompanying convergence of the San Diablo and Paraguá domains. The associated chert and BIFsupport this hypothesis, as is shown in Fig. 8d (Rizzotto et al., 2014; 2013). Noteworthy, the polarity of the subduction produced magmatism in both the Paraguá Domain and the ancient foreland (Amazonia). The San Ignacio orogeny of 1340 to 1320 Ma, represented by the PCG, aligns closely with the collisional stage of the Alto Guaporé orogeny (Rizzotto et al., 2013). These plutons are widespread over the Paraguá Domain and in a lesser amount in the San Diablo Domain (Litherland et al., 1986; Boger et al., 2005; Bettencourt et al., 2010). This means the collage between these two crustal blocks accompanied the collisional phase but was distinguished in distinct tectonic features. Whereas the Paraguá Domain is separated from the Amazonian Craton by the Trincheira ophiolite, the San Diablo front shows a major left-lateral transcurrent fault. This impingement separates the Paraguá Domain north of the San Diablo Domain in the south (Fig. 8e). The record of syn-to late-kinematic magmatism over the Paraguá Terrane and the active continental margin (Amazonia) implies continued consumption of the subducted plate below them both. The Sunsás belt is the youngest event on the SW border of the Precambrian Shield of Bolivia that produced intrusive granitic rocks such as Casa de Piedra, Taperas, Naranjito, and the Rincon del Tigre mafic-ultramafic sill, and the Huanchaca dolerite (1.11 Ga) (Fig. 8f). After this orogeny the Amazonian Craton attained tectonic stability.

In a broader geodynamic context, considering the accretionary nature of Amazonia, Ribeiro et al. (2020, 2022b) proposed an advancing episode of a Paleoproterozoic accretionary orogen combined with a retreating episode of this one. Following this point of view, the San Diablo Domain of southern Paraguá Terrane, the Western Domain of the RAT, and the Ventuari-Tapajós Province show magmatism characterized by crustal reworking produced during the advancing episode of the Paleoproterozoic accretionary orogen previously cited. The Paraguá Domain, the Eastern Domain of RAT, and the Rio Negro-Juruena province underwent crustal growth in a retreating episode of this accretionary orogen. A change of this accretionary orogen between 1596 and 1532 Ma generated the retreating of the setting. A new advancing episode in response to the convergent-to-collisional environment culminated with the collision of the RAT-Paraguá and Amazonia during the Alto Guaporé orogeny at mid-Mesoproterozoic. This convergent-to-collisional setting produced an HT metamorphism, anatexis, and crustal reworking in the Paraguá Terrane, in contrast to the HP/MT metamorphism in the RAT, suggesting a Mesoproterozoic paired metamorphic belt (Fig. 8e). The RAT-Paraguá-Amazonia connection may have lasted until at least ca. 1110 Ma, as recorded by granite magmatism and the Rincón del Tigre-Huanchaca LIP (Fig. 8f) (Teixeira et al., 2015a).

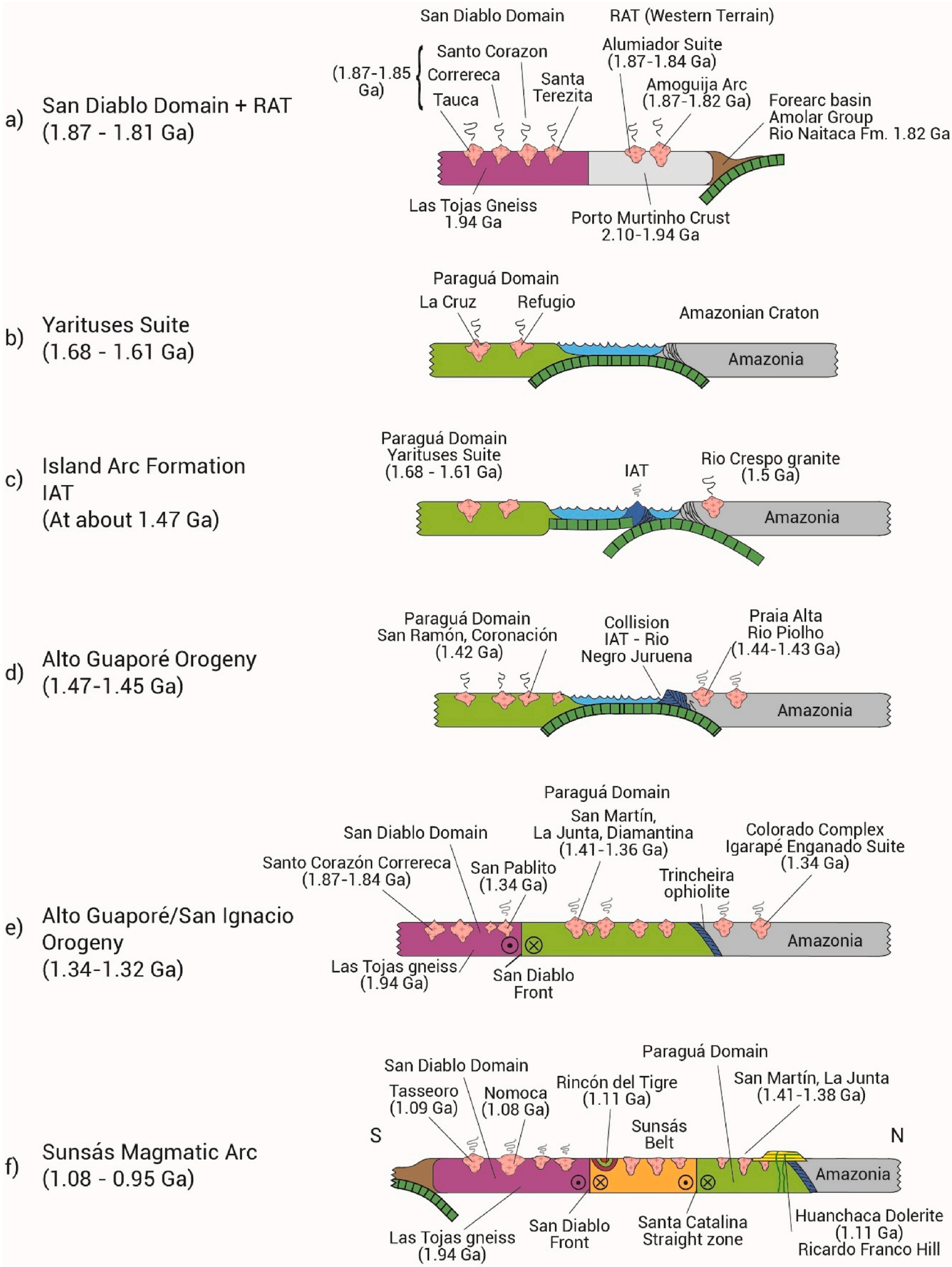

Fig. 8. Proposed tectonic models for the geological evolution of the Precambrian Shield of Bolivia (see text for explanation).

7. Conclusions

We reassessed the protracted Orosirian-Stenian evolution of the Bolivian Precambrian Shield based on new and compiled geochronology, Nd and Hf isotopes, and overviewed geological information. The data allow for a long time for new insights into the tectonic model and potential correlations with Paraguá terrane, RAT, and Amazonia. The most striking feature of the shield is the San Diablo Front which separates two domains: Paraguá and San Diablo - each with different structural and tectonic settings. On the Paraguá Domain, the LMGC is the oldest record of granulite facies gneissic rocks as old as 1818 Ma. The San Diablo Domain relates to the Las Tojas gneiss of 1941 Ma, indicative of amphibolite metamorphic facies, followed by crustal thickening at 1.87–1.85 Ga. It was juxtaposed to the Paraguá Domain during the Rondonian/San Ignacio orogeny and reactivated during the Sunsás collision. The zircon U–Pb, whole-rock Nd model ages from several granites of key places supported by field geology let us define the timing of different bodies emplaced into the Paragua terrane between 1950 Ma to 970 Ma. The Yarituses Suite crosscuts the Paraguá Domain between 1680 and 1610 Ma. Because of its regional extent, the Yarituses Suite could be used further instead of the Lomas Maneches Suite of Boger et al. (2005), which crops out locally. From a tectonic point of view, a continental arc produced the Yarituses Suite, as suggested by geochemical and isotopic constraints. According to the available geochronological knowledge, the LMGC (after Litherland et al., 1986) is the oldest unit of the Paraguá Domain. The PCG is the most representative unit of the Alto Guaporé accretional-collisional orogeny in the Bolivian shield, developed between 1.47 and 1.33 Ga (Bettencourt et al., 2010; Rizzotto et al., 2013; Ribeiro et al., 2020, 2022a, 2022b). The orogeny involved oceanic opening, arc formation, and subduction inferred here as a continental arc as part of the accretionary growth of Amazonia at the southwest of the Amazonian Craton. The geochemical and isotopic data (Fig. 5) support such a hypothesis. The available ages for the PGC, including representatives in Mato Grosso and Rondonia (Fig. 6), show that they share an evolutionary history. More precise U–Pb zircon crystallization ages fall between 1330 and 1350 Ma for the granitoid rocks, herein tentatively separated in syn-to late-kinematic to late-to post-kinematic granites of the PGC. Finally, the Sunsas allochthonous belt ends the evolution of the Amazonian Craton at the Stenian. In a broader perspective, this belt aligns with the Grenville orogeny, during which the Amazonia and Eastern Laurentia collage contributed to the formation of the Rodinia Supercontinent took place by.

CRediT authorship contribution statement

Ramiro Matos: Writing – original draft, Validation, Investigation, Data curation, Conceptualization. **Wilson Teixeira:** Writing – review & editing, Validation, Supervision, Project administration, Investigation, Funding acquisition, Formal analysis, Data curation, Conceptualization. **Amarildo S. Ruiz:** Investigation. **Jorge S. Bettencourt:** Writing – review & editing, Validation, Supervision, Formal analysis, Data curation, Conceptualization. **Mauro C. Geraldes:** Writing – review & editing, Investigation. **Gabriela Vargas-Mattos:** Methodology, Investigation. **Leticia Redes:** Investigation.

Declaration of competing interest

The authors declare that they have no known competing financial interests or personal relationships that could have appeared to influence the work reported in this paper.

Data availability

Data will be made available on request.

Acknowledgments

Ramiro Matos thanks CAPES (Coordenação de Aperfeiçoamento de Pessoal de Nível Superior) for the financial support for former his Doctoral research. Wilson Teixeira, Jorge S. Bettencourt, and Mauro C. Geraldes greatly acknowledge the support of CNPq (Conselho Nacional de Desenvolvimento Científico e Tecnológico, Brazil). We greatly thank two anonymous reviewers for their insightful comments, and very helpful suggestions, as well as Andres Folguera who efficiently handled the editorial work. The authors are indebted to Bruno V. Ribeiro for his help and fruitful revisions of the manuscript and comments that led to improvements to the paper in the knowledge of the SW Amazonian Craton.

Appendix A. Supplementary data

Supplementary data to this article can be found online at https://doi.org/10.1016/j.jsames.2023.104536.

References

Adamek, P.M., Troeng, B., Landivar, G., Llanos, A., Matos, R., 1996. Evaluación de los recursos minerales del Distrito San Ramón. Bol. Serv. Geol. Boliv. 10, 77 (La Paz).
Alcocer, R., Claure, M., 2000. Localización geofísica de nuevas áreas prospectivas para yacimientos asociados a intrusiones alcalinas en el área de Las Petas (Sudeste del Escudo Precámbrico Boliviano). Memorias del XIV Congreso Geológico Boliviano 298–302 (La Paz).
Bettencourt, J.S., Leite, W.B., Payolla, B.L., Scandolara, J.E., Muzzolon, R., Vian, J.A.J., 1997. The rapakivi granites of the Rondônia tin province, northern Brazil. In: 2nd International Symposium on Granites and Associated Mineralizations, Excursion Guide. Salvador, Bahia, Brazil, pp. 3–31.
Bettencourt, J.S., Tosdal, R.M., Leite Jr., W.B., Payolla, B.L., 1999. Mesoproterozoic rapakivi granites of the Rondônia Tin Province, southwestern border of the Amazonian Craton, Brazil–I. Reconnaissance U–Pb geochronology and regional implications. Precambrian Res. 95, 41–67.
Bettencourt, J.S., Payolla, B.L., Tosdal, R.M., Wooden, J.L., Leite Jr., W.B., Sparrenberger, I., 2006. SHRIMP-RG U-Pb zircon geochronology of gneiss of the Rio Crespo Intrusive Suite, SW Amazonian Craton, Rondonia, Brazil: new insight about protolith crystallization and metamorphic ages. In: 5th South American Symposium on Isotope Geology (Short Papers). Punta del Este, Uruguay, pp. 49–52.
Bettencourt, J.S., Leite JR., W.B., Ruiz, A.S., Matos, R., Payolla, B.L., Tosdal, R.M., 2010. The rondonian san Ignacio province in the SW amazonian craton: an overview. J. S. Am. Earth Sci. 29, 28–46.
Bettencourt, J.S., Leite JR., W.B., Payolla, B.L., 2014. Paleo-to Mesoproterozoic crustal sources for the igneous felsic rocks of the Costa Marques, Region, SW Amazonian craton, Brazil: evidence of preliminary SHRIMP U-Pb zircón ages and Hf isotopes in zircon. In: 9th South American Symposium on Isotope Geology (Abstracts). Sao Paulo, Brazil, p. 118.
Black, L.P., Kamo, S.L., Allen, C.M., Aleinkoff, J.N., Davis, D.W., Korsch, R.J., Foudoulis, C., 2003. TEMORA 1: a new zircon standard for Phanerozoic U-Pb geochronology. Chem. Geol. 200, 155–170.
Boger, S.D., Raetz, M., Giles, D., Etchart, E., Fanning, M.C., 2005. U-Pb age data of the Sunsas region of Eastern Bolivia, evidence for the allochthonous origin of the Paraguá Terrane. Precambrian Res. 139, 121–146.
Cabrera, R.F., Ruiz, A.S., Sousa, M.Z.A., Lima, G.A., Nogueira, S.F., 2009a. Caracterização Geológica Preliminar Do Granito Cascata-Complexo Granitoide Pensamiento- Terreno Paraguá-SW Do Cráton Amazônico. XI Simpósio de Geologia de Centro Oeste, Cuiabá, p. 65, 2009 (Resumos).
Cabrera, R.F., Nogueira, S.F., Ruiz, A.S., Sousa, M.Z.A., Macambira, M.J.B., Figueiredo, F.L.P., Lima, G.A., 2009b. Caracterização geológica e geocronológica (Pb-Pb) do Granito Cascata- Terreno Paraguá-SW do Cráton Amazônico. 45 Anos de Geocronologia no Brasil. São Paulo, pp. 159–161, 2009 (Resumos).
Casquet, C., Rapela, C.W., Pankhurst, R.J., Baldo, E.G., Galindo, C.M., Fanning, C.M., Dahlquist, J.A., Saavedra, J., 2012. A history of proterozoic terranes in southern south America: of Rodinia to gondwana. Geosci. Front. 3 (2), 137–145.
Compston, W., Williams, I.S., Kirschvink, J.L., Zhang, Z., Ma, G., 1992. Zircon U-Pb age of the early cambrian time-scale. Journal Geological Society of London 149, 171–184.
Cordani, U.G., Teixeira, W., 2007. Proterozoic accretionary belts in the amazonian craton. Org. In: Hatcher Jr, R.D., Carlson, M.P., McBride, J.H., Martinez Catalán, J.R. (Eds.), The 4D Framework of Continental Crust: GSA Memoir, vol. 200. Geological Society of America Book, Boulder, Colorado, pp. 297–320.
Cordani, U.G., Teixeira, W., D'Agrella-Filho, M.S., Trindade, R.I., 2009. The position of the Amazonian Craton in supercontinents. Gondwana Res. 15, 396–407.
Cordani, U.G., Fraga, L.M., Reis, N.J., Tassinari, C.C.G., Brito Neves, B.B., 2010. On the origin and tectonic significance of the intra-plate events of Grenvillian-type age in South America: a discussion. J. S. Am. Earth Sci. 29, 143–159.
Darbyshire, D.P.F., 1979. Results of the age determination program. Rep. E. Bolivia Miner. Explore. Proj. (Proyecto Precámbrico), Phase I 9 (unpublished interim report).
Darbyshire, D.P.F., 2000. The Precambrian of Eastern Bolivia – a Sm-Nd isotope study. Rio de Janeiro, Brazil. In: 31st International Geologic Congress. Abstract Volume (CD-Rom).
DePaolo, D.J., 1981. A neodymium and strontium isotopic study of Mesozoic calc-alkaline granitic batholiths of the Sierra Nevada and Peninsular Ranges, California. J. Geophys. Res. 86 (No B11), 10470–10488.
Faleiros, F.M., Pavan, M., Remédio, M.J., Rodrigues, J.B., Almeida, V.V., Caltabeloti, F. P., Pinto, L.G.R., Oliveira, A.A., Pinto de Azevedo, E.J., Costa, V.S., 2016. Zircon U-Pb ages of rocks of the Rio Apa cratonic terrane (Mato Grosso do sul, Brazil): new insights for its connection with the amazonian craton in pre-gondwana times. Gondwana Res. 34, 187–204.
Fletcher, C.J.N., 1979. La geología y potential de minerales del área de Concepción (Cuadrante SE 20-3 con parte de SE 20 - 2) (1 mapa escala 1:250.000). British

Geological Survey - Servicio Geológico de Bolivia, Santa Cruz, Bolivia, p. 73 (Open-file Report).
França, O., Ruiz, A.S., Sousa, M.Z.A., Batata, M.E.F., Lafon, J.M., 2014. Geology, petrology, U-Pb (SHRIMP) geochronology of the Morrinhos granite –Paraguá terrane, SW amazonian craton: implications for the magmatic evolution of the san Ignacio orogeny. Braz. J. Genet. 44 (3), 415–432.
Geraldes, M.C., Van Schmus, W.R., Condie, K.C., Bell, S., Teixeira, W., Babinski, M., 2001. Proterozoic geologic evolution of SW part of the amazonian craton in Mato Grosso state, Brazil. Precambrian Res. 111, 91–128.
Hawkins, M.P., 1982. The Geology and Mineral Potential of the Manomó Area (Part of Quadrangle SD 20-16), 1982. British Geological Survey-Servicio Geológico de Bolivia, Santa Cruz de la Sierra, p. 105 (Open-file Report).
Jesus, G.C., Sousa, M.Z.A., Ruiz, A.S., Matos, J.B., 2010. Petrologia e geocronologia (U/Pb-Sm/Nd) do granito Passagem, Complexo Granitoide Pensamiento, SW do Cráton Amazônico (MT). Rev. Bras. Geociencias 40 (3), 392–408.
Krogh, T.E., 1973. A low contamination method for hydrothermal decomposition of zircon and extraction of U and Pb for isotopic age determinations. Geochem. Cosmochim. Acta 37, 485–494.
Krogh, T.E., 1982. Improved accuracy of Pb/U ages by the creation of more concordant systems using an air abrasion technique. Geochem. Cosmochim. Acta 46, 637–649.
Landivar, G., Gonzalez, R., 1997. Mapa Geológico del Area Serranías San José – San Diablo. Servicio Nacional de Geología y Minería escala 1:100.000.
Leite Jr., W.B., Bettencourt, J.S., Matos, R., Payolla, B.L., Sato, K., 2016. Felsic magmatic events within 1.36 – 1.00 Ga time interval in the SW Amazonian Craton, Brazil, and Bolivia: tectonic implications and magma sources. In: 35° International Geological Congress. Cape Town, South Africa.
Litherland, M., 1982. The Geology and Mineral Potential of the Huanchaca Area (Parts of Quadrangles SD 20-15 and SD 20-11). Institute of Geological Sciences-Servicio Geológico de Bolivia, Santa Cruz, p. 173 (1 map scale 1:250,000) (Open-file Report).
Litherland, M., Annells, R.N., Appleton, J.D., Berrange, J.P., Bloomfield, K., Burton, C.C. I., Darbyshire, D.P.F., Fletcher, C.J.N., Hawkins, M.P., Klinck, B.A., Llanos, A., Mitchell, W.I., O'Connor, E.A., Pitfield, P.E.J., Power, G., Webb, B.C., 1986. The Geology and Mineral Resources of the Bolivian Precambrian Shield, vol. 9. British Geological Survey, Overseas Memoir, London, p. 153.
López-Montaño, R., y Bernasconi, A., 1988. El cinturón de rocas verdes en la hoja Concepción, Precámbrico de Bolivia Oriental: Geología, mineralización y prospección aurífera. GEOBOL-PNUD, La Paz, Informe interno, p. 43.
Ludwig, K.R., 2003. User's Manual for ISOPLOT 3.0: a Geochronological Toolkit for Microsoft Excel, vol. 4. Berkeley Geochronology Center, Special Publication, p. 71.
Marcello, A.M., Sousa, M.Z.A., Ruiz, A.S., Figueiredo, F.L.P., 2009. Aspectos petrográficos e estruturais preliminares do granito Fronteira-Complexo Granitoide Pensamiento-Terreno Paraguá-SW do Cráton Amazônico. XI Simpósio de Geologia de Centro Oeste, Cuiabá, p. 57, 2009 (Resumos).
Matos, R., 2010. Investigaciones geológicas en las provincias San Ignacio y Sunsás del Precámbrico Boliviano, una herramienta para el mapeo geológico y la interpretación tectónica de terrenos metamórficos: La Paz. Universidad Mayor de San Andrés, Trabajo de Año Sabático, p. 194.
Matos, R., 2012. Geocronología U-Pb y Sm-Nd de la Serie Yarituses y de la granodiorita San Ramón, SO del Cratón Amazónico: implicaciones para la evolución cortical del Escudo Precámbrico de Bolivia. Revista Boliviana de Geociencias 4, 33–44.
Matos, J.B., Sousa, M.Z.A., Jesus, G.C., Costa, A.C.D., Ruiz, A.S., Costa, P.C.C., Silva, C. H., Batata, M.E.F., Cabral, C., 2009. Petrología, geoquímica e geocronologia U/Pb e Sm/Nd do ortognaisse Tarumã, Fronteira Brasil/Bolivia. XI Simpósio de Geologia de Centro Oeste, Cuiabá, p. 66, 2009 (Resumos).
Matos, J.B., Sousa, M.Z.A., Ruiz, A.S., 2014. Lomas manechis granulites intrusive suite on Brazil-Bolivia border. In: A Lower Crustal Rocks of Paraguá Terrane: Petrographic, Geochemical, and U/Pb (SHRIMP) Geochronologic Constraints. 9th South American Symposium on Isotope Geology (Abstracts), p. 116.
Matos Salinas, G.R., 2010. Geocronologia e Evolução Tectônica Paleo-Mesoproterozoica do Oriente Boliviano – Região Sudoeste do Cráton Amazônico. Universidade de São Paulo, Tese de Doutorado, p. 52. + 1 mapa.
Mišković, A., Spikings, R.A., Chew, D.M., Kosler, J., Ulianov, A., Schaltegger, U., 2009. Tectonomagmatic evolution of Western Amazonia: geochemical characterization and zircon U-Pb geochronologic constraints of the Peruvian Eastern Cordilleran granitoids. Geol. Soc. Am. Bull. 121 (9/10), 1298–1324.
Mitchell, W.I., 1979. The geology and mineral potential of the Santo Corazón - Rincón del Tigre area (Quads. SE 21-5, with part of SE 21-9 and SE 21-6 with part of SE 21-10). Open file report, British Geological Survey - Servicio Geológico de Bolivia. Santa Cruz de la Sierra, p. 131 (2 maps).
Nalon, P.A., Sousa, M.Z.A., Ruiz, A.S., Macambira, M.J.B., 2013. Batólito Guaporeí: uma extensão do complexo granitóide Pensamiento em Mato Grosso - SW do Cráton Amazônico. Braz. J. Genet. 43 (1), 85–100.
Nedel, I.M., 2020. Evolução Crustal da Faixa Sunsas, Sudoeste do Cráton Amazônico. Ph. D. Thesis. Universidade de Brasília, Brasília, p. 210.
Nedel, I.M., Ruiz, A.S., Matos, R., Sousa, M.Z.A., Pimentel, M.M., Pavanetto, P., 2017. Front San Diablo na região de Miraflores, Faixa Sunsás,Bolívia: implicações tectónicas e estratigráficas. Geologia USP. Série Científica 17 (3), 125–147 (in Portuguese).
Nedel, I.M., Fuck, R.A., Ruiz, A.S., Matos, R., Ferreira, A.C.D., 2020. U-Pb geochronology and geochemistry of grenville-age plutons in the Sunsás belt - Bolivia, SW amazonian craton: tectonic and magmatic implications. J. S. Am. Earth Sci. 104, 102845.
Nedel, I.M., Fuck, R.A., Ruiz, A.S., Matos, R., Ferreira, A.C.D., 2021. Timing of Proterozoic Magmatism in the Sunsas Belt, Bolivian Precambrian Shield, SW Amazonian Craton. Geoscience Frontier, 101247.
Parrish, R.R., Roddick, J.C., Loveridge, W.D., Sullivan, R.W., 1987. Uranium-lead analytical techniques at the geochronology laboratory, geological survey of Canada. In: Radiogenic Age and Isotopic Studies: Report 1, Geological Survey of Canada, vol. 87, pp. 3–7 (2).
Quadros, M.L.E.S., Rizzotto, G.J., 2007. Geologia e recursos minerais do Estado de Rondônia: ˆ texto explicativo do mapa geológico e de recursos minerais do Estado de Rondônia. CPRM, Porto Velho. ˆ Escala 1:1.000.000.
Quadros, M.L.E.S., Giustina, M.E.S.D., Rodrigues, J.B.R., Souza, V.S., 2021. Geology and LA-ICP-MS U–Pb geochronology of the Nova Brasilândia belt, SW Amazonian Craton: new ages, re-evaluation of existing geochronological data, and implications for the evolution of the Sunsás orogeny. J. S. Am. Earth Sci. 109, 103220.
Ramos, V.A., 2009. Anatomy and global context of the Andes: main geologic features and the Andean orogenic cycle. In: Kay, S.M., Ramos, V.A., Dickinson, W. (Eds.), Backbone of the Americas: Shallow Subduction, Plateau Uplift, and Ridge and Terrane Collision, vol. 204. Geological Society of America Memoir, pp. 31–65.
Ramos, V.A., 2018. Tectonic evolution of the Central Andes from terrane accretion to crustal delamination. In: Zamora, G., Mc Clay, K.M., Ramos, V.A. (Eds.), Petroleum Basins and Hydrocarbon Potential of the Andes of Peru and Bolivia, vol. 117. American Association of Petroleum Geologist Memoir, pp. 1–34.
Ramos, V.A., Vujovich, G., Martino, R., Otamendi, J., 2010. Pampia: a large cratonic block missing in the Rodinia supercontinent. J. Geodyn. 50, 243–255.
Redes, L.A., 2021. Geologia, Geoquímica, Sm-Nd e Geocronologia U-Pb E Lu-Hf em zircão do embasamento do Oriente Boliviano: Implicações para a Evolução geodinâmica do SW/S do Cráton Amazônico. Tese de Doutorado. Universidade de Brasília, Brasília, p. 220 pp. (in Portuguese with abstract in English).
Redes, L.A., Hauser, N., Ruiz, A.S., Matos, R., Reimold, U.W., Dantas, E.L., Schmitt, R.T., Lima, B.A.F., Zacchi, E.N.P., Chaves, J.G.S., Osorio, L.F.B., Pimentel, M.M., 2020. U–Pb and Hf isotopes in granitoids of the Eastern Bolivian basement: insights into the Paleoproterozoic evolution of the western part of South America. J. S. Am. Earth Sci. 104, 102806.
Reis, N.J., Teixeira, W., D'Agrella-Filho, M.S., Bettencourt, J.S., Ernst, R.E., Goulart, L.E. A., 2021. Large igneous provinces of the Amazonian Craton and their metallogenic potential in Proterozoic times. In: Srivastava, R.K., Ernst, R.E., Buchan, K.L., de Kock, M. (Eds.), Large Igneous Provinces and Their Plumbing Systems. Geological Society, London, Special Publications, p. 518. https://doi.org/10.1144/SP518-2021-7.
Ribeiro, B.V., Cawood, P.A., Faleiros, F.M., Mulder, J.A., Martin, E., Finch, M.A., Raveggi, M., Teixeira, W., Cordani, U.G., Pavan, M., 2020. A long-lived active margin revealed by zircon U–Pb–Hf data of the Rio Apa Terrane (Brazil): new insights into the Paleoproterozoic evolution of the Amazonian Craton. Precambrian Res. 350, 105919 https://doi.org/10.1016/j.precamres.105919.
Ribeiro, B.V., Finch, M.A., Cawood, P.A., Faleiros, F.M., Murphy, T.D., Simpson, A., Stijn, G., Tedeschi, M., Armit, R., Barrote, V.R., 2022a. Of microanalysis to supercontinents: insights of the Rio Apa terrane into the mesoproterozoic SW amazonian craton evolution during Rodinia assembly. J. Metamorph. Geol. 40 (4), 631–663.
Ribeiro, B.V., Lopes, L.B.L., Kirkland, C.L., Cawood, P.A., Faleiros, F.M., Hartnady, M.I. H., Teixeira, W., Mulder, J.A., Roberts, N.M.W., Tassinari, C.C.G., 2022b. Growing the Paleo-to Mesoproterozoic margin of the SW Amazonia and the transition of an accretionary to a collisional system. Precambrian Res. 381, 106841.
Rizzotto, G.J., Hartmann, L.A., 2012. Geological and geochemical evolution of the Trincheira Complex, a Mesoproterozoic ophiolite in the southwestern Amazon craton, Brazil. Lithos 148, 277–295.
Rizzotto, G.J., Quadros, M.L., 2007. Margem Passiva e granitos Orogênicos do Ectasiano em Rondônia. In: X Simpósio de Geologia da Amazônia. Porto Velho, CDROOM.
Rizzotto, G.J., Santos, J.O.S., Hartmann, L.A., Tohver, E., Pimentel, M.M., Mc Naughton, N.J., 2013. The Mesoproterozoic Guaporé suture in the SW Amazonian craton: geotectonic implications based on field geology, zircon geochronology, and Nd-Sr isotopic geochemistry. J. S. Am. Earth Sci. 48, 271–295.
Rizzotto, G.J., Hartmann, L.A., Santos, J.O.S., McNaughton, N.J., 2014. Tectonic evolution of the southern margin of the Amazonian craton in the late Mesoproterozoic based on field relationships and zircon U–Pb geochronology. An Acad. Bras Ciências 86 (1), 57–84.
Rizzotto, G.J., Alves, C.L., Rios, F.S., Barros, M.A.S., 2019. The Nova Monte Verde metamorphic core complex: tectonic implications for the southern Amazonian craton. J. S. Am. Earth Sci. 91, 154–172.
Ruiz, A.S., 2005. Evolucão Geológica Do Sudoeste Do Cráton Amazônico, Região Limítrofe Brasil-Bolivia-Mato Grosso. State University of São Paulo, UNESP – Rio Claro, SP, Brazil, p. 260. Ph.D. thesis.
Ruiz, A.S., Matos, J.B., Sousa, M.Z.A., Lima, G.A., Macambira, M.J.B., Matos, G.R., Faria, D.A., França, O., Costa, P.C.C., 2012. Granites of Pensamiento intrusive suite: records of continental magmatic arc san Ignacio in Brazil. In: 8th South American Simposium on Isotope Geology, 2012, Medellín (Abstracts).
Santos, J.O.S., Rizzotto, G.J., Mcnaughton, N.J., Matos, R., Hartmann, L.A., Chemale Jr., F., Potter, P.E., Quadros, M.L.E.S., 2008. Age and autochthonous evolution of Sunsás orogen in west Amazon craton based on mapping and U-Pb geochronology. Precambrian Res. 165, 120–152.
Sato, K., Tassinari, C.C.G., Kawashita, K., Petronilho, L.O., 1995. Método geocronológico Sm-Nd no IG/USP e suas aplicações. An Acad. Bras Ciências 67, 313–336.
Sato, K., Tassinari, C.C.G., Basei, M.A.S., Siga Jr., O., Onoe, A.T., Souza, M.D., 2014. Sensitive high-resolution ion Microprobe (SHRIMP IIe/MC) of the institute of geosciences of the university of São Paulo, Brazil: analytical method and first results. Geol. Usp. Série Científica 14 (3), 3–14.
Scandolara, J.E., Correa, R.T., Fuck, R.A., Souza, V.S., Rodrigues, J.B., Ribeiro, P.S.E., Frasca, A.A.S., Saboia, A.M., Lacerda Filho, J.V., 2017. Paleo-Mesoproterozoic arc-accretion along the southwestern margin of the Amazonian craton: the Juruena accretionary orogen and possible implications for Columbia supercontinent. J. S. Am. Earth Sci. 73, 223–247.

Stacey, J.S., Kramers, J.D., 1975. Approximation of terrestrial lead isotope evolution by a two-stage model. Earth Planet Sci. Lett. 26 (203), 207–221.

Teixeira, W., Geraldes, M.C., Matos, R., Ruiz, A.S., Saes, G., Vargas-Mattos, G., 2010. A review of the tectonic evolution of the Sunsas belt, SW portion of the Amazonian Craton. J. S. Am. Earth Sci. 29, 47–60.

Teixeira, W., Hamilton, M.A., Lima, G.A., Ruiz, A.S., Matos, R., Ernst, R.E., 2015a. Precise ID-TIMS U–Pb baddeleyite ages (1110–1112 Ma) for the Rincón del Tigre–Huanchaca large igneous province (LIP) of the Amazonian Craton: implications for the Rodinia supercontinent. Precambrian Res. 265, 273–285.

Teixeira, W., Ernst, R.E., Hamilton, M.A., Lima, G., Ruiz, A.S., Geraldes, M.C., 2015b. Widespread ca. 1.4 Ga intraplate magmatism and tectonics in a growing Amazonia. Geosci. Front. 138, 241–254.

Teixeira, W., Hamilton, M., Girardi, V.A.V., Faleiros, F.M., 2019a. U-Pb baddeleyite ages of key dyke swarms in the Amazonian Craton (Carajás/Rio Maria and Rio Apa areas): tectonic implications for events at 1880, 1110 Ma, 535 Ma, and 200 Ma. Precambrian Res. 329, 138–155.

Teixeira, W., Reis, N.J., Bettencourt, J.S., Klein, E.F., Oliveira, D., 2019b. Intraplate Proterozoic magmatism in the Amazonian Craton reviewed: geochronology, crustal tectonics, and global barcode matches. In: Rajesh (Ed.), Dyke Swarms of the World-A Modern Perspective. Springer Geology, pp. 111–154. https://doi.org/10.1007/978-981-13-1666-1_4.

Teixeira, W., Cordani, U.G., Faleiros, F.M., Sato, K., Maurer, V.C., Ruiz, A.S., Azevedo, E. J.P., 2020. The Rio Apa Terrane reviewed: U Pb zircon geochronology and provenance studies provide paleotectonic links with a growing Proterozoic Amazonia. Earth Sciences Review 202, 103089. https://doi.org/10.1016/j.earscirev.2020.103089.

Tohver, E., van der Pluijm, B.A., Mezger, K., Scandolara, J.E., Essene, E., 2005. Two-stage tectonic history of the SW Amazon craton in the late Mesoproterozoic: identifying a cryptic suture zone. Precambrian Res. 137, 35–59.

Tohver, E., Teixeira, W., van der Pluijm, B.A., Geraldes, M.C., Bettencourt, J.S., Rizzotto, G., 2006. Restored transect across the exhumed Grenville orogen of Laurentia and Amazonia, with implications for crustal architecture. Geology 34, 669–672.

Vargas-Mattos, G., 2010. Caracterização Geocronológica e Geoquímica dos Granitos Proterozóicos na Bolívia: Implicação para à Evolução Crustal da Borda SW do Cráton Amazônico na Bolívia. Universidade do Estado do Rio de Janeiro, Tese de Doutorado, Rio de Janeiro, p. 165.

Vargas-Mattos, G., Geraldes, M.C., Matos, R., Teixeira, W., 2010. Paleoproterozoic Granites in Bolivian Precambrian Shield: the 1.92-1.89 Ga Correreca Magmatic Rocks and Tectonic Implications. South American Symposium on Isotope Geology, Brasília, 2010 (Short Papers).

Vargas-Mattos, G., Geraldes, M.C., Tavares Jr., A.D., Matos, R., Teixeira, W., 2020. Petrografia, geoquímica e geocronologia das rochas graníticas da orogenia San Ignácio (Bolívia). Revista UNESP Geociências 39 (1), 1–19.

Witschard, F., Matos, R., Nilsson, L., 1993. Airborne geophysical survey and interpretations of remote sensing in the san Ramon area. In: Boletín del Servicio Geológico de Bolivia, No.2 (Especial), p. 55. La Paz.